Liquefaction and Other Ground Failures in Imperial County, California, from the April 4, 2010, El Mayor–Cucapah Earthquake

By Timothy P. McCrink, Cynthia L. Pridmore, John C. Tinsley, Robert R. Sickler, Scott J. Brandenberg, and Jonathan P. Stewart

Liquefaction-triggered ground failure in Fig Lagoon levee. Scarps indicate probable differential subsidence into a liquefied substrate. Photograph by John Tinsley.

Pamphlet to accompany

U.S. Geological Survey Open-File Report 2011–1071

California Geological Survey Special Report 220

2011

U.S. Department of the Interior
U.S. Geological Survey

State of California

EDMUND G. BROWN JR.

Governor

The Resources Agency

JOHN LAIRD

Secretary for Resources

Department of Conservation

DEREK CHERNOW

Acting Director

California Geological Survey

JOHN G. PARRISH, Ph.D. State Geologist

U.S. Department of the Interior
KEN SALAZAR, Secretary

U.S. Geological Survey
Marcia K. McNutt, Director

U.S. Geological Survey, Reston, Virginia 2011

For product and ordering information:
World Wide Web: http://www.usgs.gov/pubprod
Telephone: 1-888-ASK-USGS

For more information on the USGS—the Federal source for science about the Earth, its natural and living resources, natural hazards, and the environment:
World Wide Web: http://www.usgs.gov
Telephone: 1-888-ASK-USGS

Suggested citation:
McCrink, T.P., Pridmore, C.L., Tinsley, J.C., Sickler, R.R., Brandenberg, S.J., and Stewart, J.P., 2011, Liquefaction and other ground failures in Imperial County, California, from the April 4, 2010, El Mayor–Cucapah earthquake: U.S. Geological Survey Open-File Report 2011–1071 and California Geological Survey Special Report 220, 94 p. pamphlet, 1 pl., scale 1:51,440. [http://pubs.usgs.gov/of/2011/1071/] [*http://conservation.ca.gov/cgs*]

Author Affiliations

Timothy P. McCrink and Cynthia L. Pridmore, California Geological Survey (Sacramento, Calif.)

John C. Tinsley and Robert R. Sickler, U.S. Geological Survey (Menlo Park, Calif.)

Scott J. Brandenberg and Jonathan P. Stewart, University of California, Los Angeles

Conversion Factors

Multiply	By	To obtain
	Length	
centimeter (cm)	0.3937	inch (in.)
meter (m)	3.281	foot (ft)
kilometer (km)	0.6214	mile (mi)
hectare (ha)	2.471	acre

Altitude, as used in this report, refers to distance above the vertical datum.

Table of Contents

Plate

Figures

Tables

Executive Summary

The moment magnitude (M_w)7.2 mainshock of the Sierra El Mayor–Cucapah earthquake occurred at 3:40 pm local time (22:40:42 universal time coordinated) on April 4, 2010. The epicenter was located in the southern Mexicali Valley at the foot of the Sierra El Mayor and Sierra Cucapah. The seismogenic fault rupture propagated both northwesterly into the mountains and southeasterly toward the Gulf of California for a total surface rupture length of approximately 120 kilometers. Near-field strong motion recordings, with stations located entirely east and north of the fault rupture, measured peak ground accelerations of 0.40 to 0.54 g in the lower Mexicali Valley. North of the international border, peak ground accelerations were recorded at 0.59 g southwest of El Centro, 0.38 to 0.56 g in El Centro, and 0.27 g in Calexico.

Extensive slope failure in the Sierra Cucapah was indicated by large volumes of dust immediately following the earthquake. No other earthquake-triggered bedrock slope instability has been reported from Mexico, though a small-displacement landslide was triggered by a M5.7 aftershock in the Yuha Basin west of Imperial Valley (J. Treiman, California Geological Survey, 2010, oral commun.). Agricultural and transportation infrastructure was severely damaged by extensive liquefaction in the Mexicali Valley with damage estimated in the hundreds of millions of dollars. Liquefaction deformation was also responsible for severe damage to residential buildings along the Rio Hardy, and settlement-related damage to buildings at the Universidad Autónoma de Baja California in Mexicali, which was constructed on young sediments deposited by the New River. In Imperial County, California, the focus of this report, considerable liquefaction-related damage also occurred, though not nearly as widespread as in Baja California. Relatively minor occurrences of nonliquefaction slope instability were triggered by this earthquake in Imperial County.

Field observations of earthquake-triggered ground failures in Imperial County as reported here were carried out by teams from the University of California, Los Angeles, the U.S. Geological Survey, and the California Geological Survey. These teams investigated 138 sites during an 8-day period, and 63 of these were found to have sufficient damage to warrant detailed description in this report (summarized in table 1, Principal Sites). The sites described here are categorized by the cultural facility (for instance, roads and bridges) or natural features (for instance, drains and rivers) most affected by liquefaction-related ground failure, or, in the case of nonliquefaction slope failures or other indications of strong shaking, by the nearest cultural facility.

Roads and Bridges

Most road closures in Imperial County were confined to bridge crossings of the New River and its tributary drainages. These road closures were often related to liquefaction of bridge approach fills or the underlying Holocene alluvial soils resulting lateral spreading and settlement of fill relative to the bridge structures. This sequence of events was the case where Drew, Brockman and Worthington roads cross the New River. Lateral spreading occurred within access road fill and for several hundred meters along the west bank of Greeson Drain south of Lyons Road. Where Lyons Road crosses the New River, liquefaction-induced lateral spreading occurred in natural soils and in road fills 100 meters northeast and 200 meters southwest of the bridge, yet the bridge structure and approach fills were apparently undamaged. The westbound on-ramp from Drew Road onto Interstate Highway 8 was damaged by settlement and slumping of highway fills. Vented sand and lateral spreading fissures on the adjoining New River floodplain strongly suggest that liquefaction was the cause of the highway damage. Austin Road was closed for a time between Interstate Highway 8 and McCabe Road, and a small, possibly liquefaction-related, slump toward

the Central Main Canal was found 150 meters north of McCabe Road. No evidence of liquefaction or other strong shaking effects were found on any of the bridge crossings of the Alamo River from State Highway 98 north to Rutherford Road and Weist Lake.

Irrigation Canals

Most damage to irrigation canals was concentrated along the Westside Main Canal, which runs along the western edge of the irrigable land of the Imperial Valley. The canal did not completely fail in any location, but substantial liquefaction-related damage affected embankments, levees, and diversion structures at many points between the All American Canal on the south and Huff Road on the north. Liquefaction at the base of power poles and the foundation of a small utility shed accompanied incipient lateral spreading at the diversion of the Westside Main Canal from the All American Canal. The All American Canal generally performed well, but it experienced some damage inferred to be related to liquefaction. Small slumps thought related to liquefaction were observed along the All American Canal at the Woodbine Lateral and both east and west of the Alamo River. There was a damaging lateral spread of the west bank of the Wistaria Canal just north of its diversion from the All American Canal. Liquefaction accompanied by lateral spreading occurred on both sides of the Rosita Canal northwest of Holtville, disrupting the levees and allowing seepage onto adjacent agricultural fields. Nichols Road was closed south of Evan Hewes Highway owing to large volumes of water being splashed out of the Eucalyptus Canal onto the road. A similar large splash out of this canal was found on Nichols Road from 50 to 150 meters north of McCabe Road.

Drains and Rivers

In addition to the previously noted damage to roads that cross the New River, liquefaction and related effects were observed elsewhere at several locations along the New River and some of its tributary drains. Fig Lagoon is a 37 hectare (92 acre) body of water south of Interstate Highway 8 separated from the New River by a 1,500-meter-long levee. Liquefaction effects on this levee included vented sand and lateral spread slumps and fissures. In one place, a slump block dropped enough to allow earthquake-generated seiche waves to overtop the levee and flow into the New River, lowering the lagoon water level by 0.3 to 0.5 meters and flooding the natural flood plain to the east and north of the lagoon. Fortunately, neither the slump block nor erosion caused by the overtopping flow permanently breached the levee. Vented sand and lateral spreading also occurred along the New River southeast of Fig Lagoon and west of Drew Road, and nonliquefaction slumping and soil toppling blocked dirt roads along Fig Drain south of Fig Lagoon. A large (80 by 90 meters) lateral spread occurred in the southwest corner of an agricultural field along Rice Drain No. 3, immediately north of Evan Hewes Highway and west of Forrester Road. The farthest northward inferred occurrence of liquefaction was a moderate-size slump into Cook Drain along Fites Road. The presence of seepage from the Westside Main Canal appears to have created a saturated soil condition that increased the potential for liquefaction. Liquefaction along the Alamo River was confined to relatively minor, incipient slumps with no vented sand in the area just north of the All American Canal.

Major Facilities and Earthen Dams

New River sediments liquefied at many locations in the floodplain in Calexico, from the International Border to the All American Canal aqueduct. Lateral spreading caused considerable damage at the Calexico Waste Water Treatment Plant, which lies on the south bank of the New River floodplain, immediately north of the Calexico Airport. The access road east of the plant,

which has sewer lines running beneath it, was severely disrupted by lateral spreading, as were treatment pond levees on the west side of the plant. An underground 91-centimeter-diameter sewer line that feeds the treatment plant ruptured where it emerges from the ground and crosses the New River north of the plant. On the basis of the extent of lateral spreading in this area, the rupture may have been influenced by liquefaction. Less than a kilometer downstream, vented very fine sand and lateral spread slumps were observed at and around the foundation structures for the All American Aqueduct, though no discernable damage to the structure was found. The timber bridge across the New River, 75 meters upstream from the aqueduct, was closed by the earthquake. Liquefaction settlement and lateral spreading severely damaged the dam embankment and outlet works for Sunbeam Lake, a county-run recreational facility, and caused major damage to Drew Road. Water flowing around the damaged lake outlet pipes resulted in the formation of a large sinkhole on the dam crest that threatened the dam's integrity and forced an emergency repair less than two weeks after the earthquake. As of September 15, 2010, Drew Road west of Sunbeam Lake was still closed and awaiting repairs.

Conclusions

Liquefaction and its related effects damaged numerous roads, bridges, levees, and dams throughout the southwestern third of Imperial County. Most liquefaction was concentrated along the Westside Main Canal and the New River, which are the waterways closest to the seismic sources in the Sierra Cucapah. However, liquefaction occurrences were found as far east as Holtville and are inferred to have occurred as far north as Fites Road south of Brawley where the susceptibility is assumed to have been high. A list of the principal sites that experienced liquefaction or other earthquake effects is provided in table 1.

The frequency and intensity of damage generally decreased to the north and east, away from the earthquake epicenter and the sediment source, the Colorado River. This trend likely reflects the attenuation of strong ground motion with increasing distance from the earthquake source as well as a tendency for natural deposits to exhibit increased content of fines (silt and clay) away from the Colorado River. One occurrence of liquefaction and lateral spreading in an agricultural field documented in this reconnaissance appears to be related to the absence of tile drains. Tile drains are common features in most agricultural fields in Imperial County, where few fields experienced liquefaction, but are less common in the Mexicali Valley where extensive liquefaction-related damage was observed. The extent to which tile drains reduce surface manifestations of liquefaction and under what conditions should be studied further.

Few sites that experienced liquefaction during the El Mayor–Cucapah earthquake experienced liquefaction in previous earthquakes in the Imperial Valley. Liquefaction at the Worthington Road crossing of the New River, the farthest north found along the New River in this reconnaissance, also was reported during the 1968 Borrego Mountain and 1987 Superstition Hills earthquakes. Inferred liquefaction-related slumping along the Westside Main Canal triggered by this earthquake occurred in similar areas with similar styles of deformation as failures reported from the 1987 Superstition Hills earthquake. Finally, extensive cracking and slumping along the All American Canal at the Alamo River crossing observed in this reconnaissance was also reported during the 1987 Superstition Hills and 1979 Imperial Valley earthquakes.

Table 1. Principal sites investigated during postearthquake reconnaissance in Imperial County. *A*, Liquefaction was confirmed at the site or sites by the presence of vented sand. *B*, Vented sand was not found, but the nature of the deformation observed is consistent with liquefaction. *C*, Sites where ground deformation typically is in the form of minor ground cracking (a few millimeters of displacement) liquefaction is possible, but not necessary to explain the deformation. *D*, Nonliquefaction ground failure, usually shallow slope failures. *E*, Sites where clear evidence for the development of seiche waves was found. *F,* Sites where structural or cultural features showed evidence of strong shaking independent of liquefaction or other ground failure (for example, soil pushed away from structures such as bridge abutments). As used here, a "site" is typically an aggregation of a number of individual observations or global positioning system–located "way points." Depending on the extent of earthquake damage, a site can cover a relatively large area, and some parts may have clear evidence of liquefaction while other parts have less clear or no evidence. Thus, more than one column can be checked for any given site on this summary table.

	Liquefaction				Other	
Principal Site Name (alphabetical listing)	A Confirmed	B Inferred	C Possible	D None Found	E	F
	Liquefaction - Vented Sand	Lateral Spread, Slump, Settlement - No Vented Sand	Minor Cracking, Lateral Extent Variable	Slope Failure or Settlement - Not Liquefaction	Seiche	Evidence of Strong Shaking
All American Canal (WMC to the Alamo River)		X	X	X		
All American Canal Aqueduct over the New River	X	X	X			X
Brockman Road at Greeson Drain		X				X
Brockman Road at the New River		X				X
Calexico Waste Water Treatment Plant	X	X				X
Central Main Canal north of McCabe Road		X	X	X		
Central Main Canal south of Interstate Highway 8			X	X		
Cook Drain at Fites Road		X				
Drew Road at the New River	X	X				X
Eucalyptus Canal north of McCabe Road					X	
Eucalyptus Canal south of Evan Hewes Highway					X	
Evan Hewes Highway at the New River				X		
Fig Drain south of Fig Lagoon				X		
Fig Lagoon and the New River	X	X			X	
Forrester Road at the New River			X	X		
Hetzel Road at Salt Creek Drain			X			X
Interstate Highway 8 at the New River	X	X				
Keystone Road at the New River				X		
Lyons Road at Greeson Drain		X	X			
Lyons Road at the New River	X	X				X
New River Flood Plain 550 m west of Drew Road		X				
Rice Drain No.3 at Evan Hewes Highway	X	X				
Rio Bend RV Park Lake and Golf Ranch	X	X				
Rosita Canal north of Bell and Alamo Roads	X	X				
State Highway 86 at the New River			X			X
Sunbeam Lake Dam and Drew Road	X	X	X		X	
Westside Main Canal (AAC to Huff Road)	X	X	X	X		
Worthington Road at the New River	X	X		X		X

Introduction

The moment magnitude (M_w)7.2 El Mayor–Cucapah earthquake struck at 22:40:42 Universal Time Coordinated (UTC) or 3:40 pm local time on Easter Sunday, April 4, 2010. The mainshock had an estimated focal depth of 10 kilometers (km) (U.S. Geological Survey, 2010) and originated northeast of the Sierra El Mayor and southeast of the Sierra Cucapah, southwest of Mexicali, Baja California, Mexico. The epicenter was located at 32.237°N, 115.083°W (U.S. Geological Survey, 2010). The earthquake was felt throughout northern Baja California and southern California, and caused damage in a region from the Sea of Cortez in the south to the Salton Sea in the north (fig. 1). The El Mayor–Cucapah earthquake is the largest to strike this area since 1892. The mainshock was followed by a sequence of aftershocks concentrated in the northern Laguna Salada and Yuha Basin areas and culminated with a M_L5.7 earthquake on June 14 near the town of Ocotillo.

The USGS instrumental intensity was IX near the fault rupture, and VIII in Mexicali, which is the nearest densely populated area (U.S. Geological Survey, 2010). The largest peak ground acceleration of 0.59 g was recorded at McCabe School about 5 km southwest of El Centro, California (fig. 2). The 140-km-long surface rupture extended from the northern tip of the Sea of Cortez northwestward to nearly the international border, with strike-slip, normal, and oblique displacements observed. The earthquake caused two fatalities and hundreds of injuries. Damage occurred to irrigation systems, water treatment facilities, buildings, bridges, earth dams, and roadways. Liquefaction and ground subsidence was widespread in the Mexicali Valley, and they left wheat and hay fields submerged under water. They also destroyed many canals that irrigate fields in the predominantly agricultural region. The largest effect of the earthquake was its damage to agricultural infrastructure (including levees and canals) in the Mexicali Valley. This damage is anticipated to cost hundreds of millions of dollars to repair (R. Anderson, California Seismic Safety Commission, 2010, written commun.). The earthquake has provided important lessons regarding water infrastructure in seismically active regions.

The Imperial Valley, the focus of this report, also experienced liquefaction and related ground deformation, but these effects were not nearly as widespread as in the Mexicali Valley. As a result, the estimated damage costs are about $50 million in Imperial County, an order of magnitude lower. Ground motions well in excess of those needed to induce liquefaction were experienced in much of southern Imperial County. Therefore, the primary reasons for this difference in liquefaction extent and damage is currently attributed to the generally lower groundwater table and finer grained, primarily lacustrine sediments underlying the majority of the agricultural uplands, compared with the shallow groundwater and coarser grained fluviatile sediments of the Colorado River delta in the Mexicali Valley. There is some indication from this reconnaissance that the ubiquitous use of tile drains in Imperial County agricultural practice may have prevented surface manifestations of liquefaction, but this potentially beneficial effect of tile drains needs to be confirmed by more detailed study.

Within one to four days following the earthquake, the University of California, Los Angeles (UCLA), the United States Geological Survey (USGS), and the California Geological Survey mobilized field personnel in order to document and locate effects of earthquake-triggered liquefaction in Imperial County, California. The reconnaissance lasted a little more than one week and concentrated on readily accessible locations, chiefly along roads, principal irrigation canals and drains, and along reaches of the New and Alamo Rivers. The observations presented in this report represent a fairly comprehensive picture of the distribution and nature of liquefaction associated with this event.

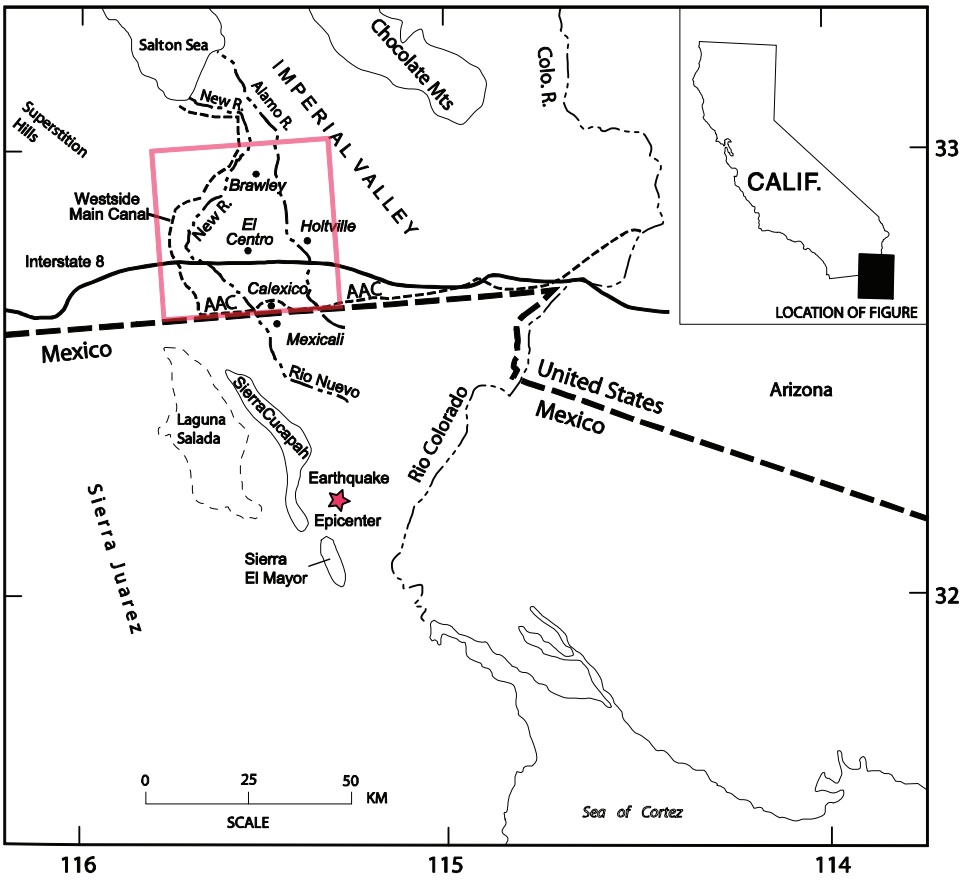

Figure 1. Area affected by the El Mayor–Cucapah earthquake and the area covered by this reconnaissance report (red box). The All American Canal (AAC), the Westside Main Canal, the New River, and the Alamo River are depicted with dashed lines. Major cities are indicated.

Tectonic Setting and Areal Geology

The Imperial Valley lies in the Salton Trough, a geologically young structural and topographic depression that is the northern extension of the Gulf of California. The Salton Trough formed in the complex transition zone from oceanic ridge spreading of the East Pacific Rise, which dominates the tectonics of the Gulf of California, to the continental transform boundary represented by the San Andreas fault. In this transition zone, extension between right-lateral strike-slip fault segments results in the formation of pull-apart basins (Brothers and others, 2009). The strike-slip faults that bound or traverse the Imperial Valley include, from east to west, the San Andreas, Imperial, San Jacinto, and Elsinore fault zones. The fault that is regarded as the primary continuation of the San Andreas fault in the Imperial Valley is the Imperial fault with an associated step-over represented by the Brawley seismic zone south of Salton Sea. In turn the Imperial fault steps over to the Cerro Prieto fault in Mexico, and the corresponding extensional pull-apart basin underlies the Mexicali Valley. The faults that ruptured in the El Mayor–Cucapah earthquake lie west of the Cerro Prieto fault and include the newly named Indiviso fault underlying the Colorado River delta to the south, the Pescadores fault in the southern Sierra Cucapah, and the Borrego fault in the northern Sierra Cucapah. While the Indiviso fault exhibited primarily right-lateral strike-slip displacement, the Pescadores and Borrego faults showed both strike-slip and normal, down-to-the-east displacements. A small segment of the Laguna Salada fault, considered the southern extension

of the Elsinore fault zone on the west side of the Sierra Cucapah and which also ruptured in this earthquake, had normal, down-to-the-west displacements. Thus, the El Mayor–Cucapah earthquake exhibited both transform and extensional fault ruptures in this complex tectonic transition zone.

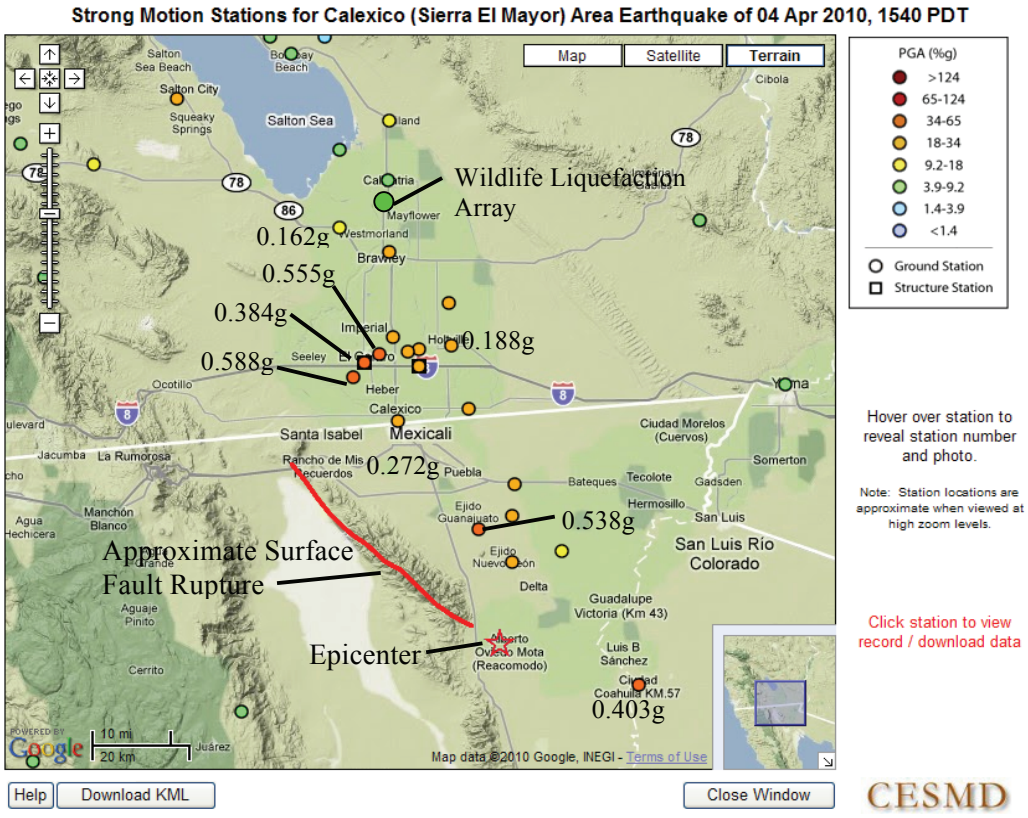

Figure 2. Strong ground motion seismograph stations recording the 4/4/2010 El Major–Cucapah main shock in the Imperial Valley and Mexicali Valley areas. Stations colored according to recorded levels of peak horizontal ground acceleration. Highest recorded levels bracket Interstate 8 north and west of Calexico. No stations exist along the western margin of the southern Imperial Valley. This map and the posted peak acceleration values were obtained from the Center for Engineering Strong Motion Data (CESMD; *http://www.strongmotioncenter.org/*). Last accessed October 20, 2010.

As the Imperial and Coachella Valleys subsided in response to extensional tectonics during the Pliocene and Pleistocene, roughly 6,100 meters (m) of sediment was deposited. Coarse-grained sediment at the basin margins was derived from surrounding crystalline basement rocks, and finer grained sediments in the central parts of the basin were derived largely from the Colorado River (Merriam and Bandy, 1965). The Holocene depositional history of Imperial Valley also is dominated by the influence of the Colorado River. While currently flowing south to the Gulf of California, this major river has intermittently flowed north, depositing sediments and filling the northern Salton Trough with freshwater lakes. Ancient Lake Cahuilla, first recognized and named by William Phipps Blake in 1857, last covered this area approximately 300 to 400 years ago (Sharp, 1981). In southern Imperial Valley, fine-grained lake deposits are interbedded with coarse-grained stream channels and deltaic deposits. These sand deposits east of Calexico and west of the Alamo River are thought to have strongly influenced the location of liquefaction occurrences during the 1979 Imperial Valley earthquake (Youd and Wieczorek, 1982). Similar-textured soils have been identified on the east and west sides of the valley floor, most significantly for this report along the Westside Main Canal (Strahorn and others, 1922).

Much of the Imperial Valley lies below sea level, and the lowest part is occupied by the Salton Sea. This body of water is the result of uncontrolled levee failures along the Colorado River in Mexico from 1905 to 1907 (Mendenhall, 1909). Prior to that time, historical accounts report that the valley was dry with occasional floods from the New and Alamo Rivers, which would produce an ephemeral shallow body of water in what was known as the Salton Sink (Blake, 1857; Cory and Blake, 1915). The repeated flooding and incision of the New and Alamo Rivers into the Holocene lacustrine deposits of Lake Cahuilla left behind loose, granular sediments that are susceptible to liquefaction in the floodplains of these modern rivers. Flooding events of the New and Alamo Rivers in the last 100 years, though not as dramatic as in 1905 to 1907, reworked and redistributed these deposits. Irrigation runoff from agricultural fields provides a nearly continuous source of flowing water for these rivers and their tributary drains.

Historic Seismicity and Related Ground Failures

Strong earthquake shaking and the occurrence of liquefaction are recurring themes in the Imperial and Mexicali valley areas. The following is a brief history of liquefaction-related effects associated with major earthquakes in this region:

1852 and 1892 Early descriptions of possible liquefaction in the Imperial–Mexicali Valley region are associated with the November 29, 1852 (M_L6.5; most magnitudes reported here are from the Southern California Earthquake Center) and February 23, 1892 (M_w7.1) earthquakes. The 1852 earthquake was centered near Volcano Lake in Baja California and triggered activity in the mud volcano area near the lake shoreline (Beal, 1915). Adjacent to the Colorado River near Fort Yuma (now Winterhaven), fissures produced sand and water from the banks and adjacent alluvial plain (Stover and Coffman, 1993). The 1892 earthquake is known to have ruptured the Laguna Salada fault in Baja California (Mueller and Rockwell, 1995), and it produced reports of ground sinking near El Centro, great fissures appearing on the desert floor northwest of Yuma, and "wet ground cracked" in the Moreno Valley area of Riverside County. As with the 1852 earthquake, the 1892 earthquake generated reports of groundwater ejected in Volcano Lake (Hough and Elliot, 2004). Southern Imperial Valley was largely uninhabited until 1900, and no reports of ground failure are known for earthquakes prior to that time.

1915 On June 22, 1915, a M_L6.3 earthquake occurred in the Imperial Valley, centered near Heber (Beal, 1915). This earthquake was preceded by a strong foreshock one hour earlier. Reports indicate that the banks of the New River northwest of El Centro sank a few inches to more than a foot and that water flowed from cracks for some time. The Alamo River also had bank failures. Additional settling associated with liquefaction is inferred from reports that farms required one third more water, and many holes were found in fields after the event. Cracks formed in alluvium parallel to levees in the Imperial Valley, but only minor damage to the irrigation ditches occurred (Stover and Coffman, 1993).

1915 On November 20, 1915, a M_S7.1 earthquake jolted northern Baja California and Imperial Valley. Large, deep cracks developed in the levees at Volcano Lake and along the New River. Mud and steam were ejected from the Volcano Lake area (Stover and Coffman, 1993).

1930 On February 25, 1930, a M5.7 earthquake centered near Westmorland produced "craterlets," and mud and water were forced from the ground east of the town (Youd and Wieczorek, 1984; Stover and Coffman, 1993).

1940 On May 18, 1940, the M_w6.9 Imperial Valley earthquake caused widespread damage to the Imperial and Mexicali Valleys. Numerous sand boils, craters, cracks, and associated geysers spouting water several feet high were reported throughout the lower Colorado River area (Sylvester, 1979). Railroad tracks settled from just south of Brawley to the border and in Mexico east to the Colorado River (Ulrich, 1941). Extensive cracking, slumping, and lurching of canals and

saturated river banks were reported (Sylvester, 1979). Damage to irrigation canals was widespread. Breaks occurred along almost the entire length of the Ash Canal from Holtville south to the border. In Mexico both banks of the Central Main and the Alamo Canals were broken for a distance of 25 miles. Numerous sand boils and water geysers were reported near Gadsden (Stover and Coffman, 1993).

1950 During July and August 1950, several earthquakes as much as M_L5.4 shook the areas around the cities of Calipatria and Westmorland. Two of these events generated numerous sand boils and fissures along the Vail Canal southwest of Calipatria (Youd and Wieczorek, 1984). Near Calipatria, many sand boils were formed and the ground settled and cracked (Stover and Coffman, 1993).

1953 On June 13, 1953, a M_L5.5 earthquake shook the Brawley area. Some canals developed cracks, and settlement occurred along the banks (Stover and Coffman, 1993).

1957 On April 25, 1957, a M_L5.2 earthquake shook the Calipatria and Westmorland areas, producing hundreds of sand boils and cracks in an area approximately 7 miles west of Calipatria (Youd and Wieczorek, 1984; Stover and Coffman, 1993).

1968 On April 9, 1968, the M_w6.5 Borrego Mountain earthquake occurred on a 30 km segment of the Coyote Creek fault, a southern branch of the San Jacinto fault system west of Imperial Valley. Small sand boils associated with landward slumps were reported along the New River at the Worthington Road Bridge, approximately 55 km southeast of the epicenter, and sand boils were observed at the margins of recently irrigated fields near the epicenter (Castle and Youd, 1972). In addition, a 125-m-long slump of the east New River bluff occurred west of the town of Seeley, offsetting Evan Hewes Highway by 5 centimeters (cm) (Castle and Youd, 1972).

1979 On October 15, 1979, the M_W6.4 Imperial Valley earthquake occurred on the northern 30 km of the Imperial fault, or about half of the length of the 1940 fault break (Ellsworth, 1990). Liquefaction, ground failure, and other secondary effects occurred within the flatlands associated with the New and Alamo Rivers, and within embankments along canals, rivers and highways (Youd and Wieczorek, 1982). The Ash, All-American, and East Highline Canals were damaged. Most of the liquefaction effects were within 4 km of the fault rupture, and the most distant effects were at a distance of 16 km (Youd and Wieczorek, 1982).

1980 On June 9, 1980, a M6.1 earthquake occurred near Guadalupe Victoria, Baja California. The earthquake caused fissures, sand boils, and small craters. Leveling surveys indicated as much as 55 cm of subsidence (Zelwer and Grannell, 1982).

1981 On April 26, 1981, a M_L5.8 earthquake centered near Westmorland produced liquefaction and other secondary effects in several localities within a 150 square km area north of Westmorland. These effects included sand boils, fissures, slumps, lateral spreads, ground settlement, and fields spotted with sand, and disrupted fields, roads, and canals. Most of the liquefaction sites were within 7 km of the estimated seismic source zone, with the exception of one site located 12 km away (Youd and Wieczorek, 1984).

1987 On November 23 and 24, 1987, two large earthquakes, M_W6.2 and M_W6.6, respectively, shook Imperial County. The first earthquake occurred on a northeast-trending, left-lateral strike-slip fault that intersected the northwest-trending, right-lateral Superstition Hills fault, which subsequently ruptured and produced the second earthquake (Ellsworth, 1990). Extensive liquefaction occurred at the Wildlife Liquefaction Array near Calipatria, the first test of this unique facility (Holzer and others, 1989). Liquefaction occurred in approach fills on both sides of the Worthington Road Bridge across the New River, requiring replacement of the bridge (Meehan and others, 1988). Extensive damage to irrigation canals and other facilities occurred throughout southern Imperial Valley (Finch, 1988). Roughly 600 m of cracked dirt embankment and several "slip-outs" were reported along the Westside Main Canal northwest of the Fern Canal diversion.

Vented sand was found along the All American Canal just southwest of the New River. Slump cracks along the All American Canal were reported extending to the Sand Hills on the east side of Imperial Valley (Finch, 1988).

Ground Motion and Liquefaction Occurrence

Peak ground accelerations from selected strong ground motion stations for the April 4, 2010, El Major–Cucapah mainshock in the Imperial and Mexicali Valleys are shown in figure 2. The instrumental array recorded peak horizontal ground acceleration (PGA) values as high as 0.58 g (at McCabe School, west of El Centro), with a number of stations in the El Centro area recording PGA values exceeding 0.25 g. At more distant sites, 0.19 g was recorded at the Holtville Post Office, and 0.16 g at the Westmorland Fire Station (beyond the geographic limit of observed liquefaction). No stations currently exist in the vicinity of the Westside Main Canal where much liquefaction occurred.

The effects of this event can be compared with the 1989 northern California Loma Prieta earthquake (M_W6.9) where PGA values associated with the distal limit of liquefaction (in active channel deposits) occurred at, or slightly above, 0.12 g. The Imperial Valley appears to have required a higher acceleration to develop surface expression of liquefied materials.

Figure 3 shows the general distribution of observed ground failure effects. Liquefaction-related ground failure and associated permanent ground deformation were most common in the southwestern portion of the Imperial Valley, with a notable exception located northwest of the town of Holtville (right-center of fig. 3). Lateral spreading, ground cracking, differential settlement and vented sand ("sand blows" or "sand boils") were commonly noted. All locations of reported liquefaction from the 1979 M6.9 Imperial Valley earthquake inspected in this reconnaissance were found to not have experienced liquefaction during this earthquake, with the possible exception of small slumps along the All American Canal just east of the Alamo River (Youd and Wieczorek, 1982*, their* fig. 171).

The Wildlife Liquefaction Array (WLA), located on the floodplain of the Alamo River near the City of Calipatria (fig. 2), was established in 1982 at a site where liquefaction occurred during the 1981 Westmorland earthquake (Youd and Wieczorek, 1982). The original array, modified in 2004 and 2005, contains accelerometers at the ground surface, at 30 m depth, and at 100 m depth and pore-pressure transducers at several depths in the liquefiable sand layer. Liquefaction recurred at this site during the 1987 Superstition Hills earthquake, and the event has been evaluated and documented in great detail (Holzer and others, 1989; Holzer and Youd, 2007). Liquefaction did not recur at the WLA site during the El Mayor–Cucapah earthquake. Peak accelerations of about 0.1 g above the liquefiable sand layer and 0.08 g below the sand layer were recorded at WLA during this earthquake. In addition, pore pressures were elevated to <20 percent of the overburden stress within the liquefiable layer, and liquefaction was not initiated (J. Steidl, University of California, Santa Barbara, 2011, written commun.).

Field Observations

Research teams from three organizations deployed to the field following the April 4, 2010, El Mayor–Cucapah earthquake. A team from the University of California, Los Angeles (UCLA) was in southern Imperial County on April 5, and—notably—this team was able to document shaking damage to the All American Canal before it was altered by repair crews. The UCLA team continued their reconnaissance in Mexico on April 6. The U.S. Geological Survey sent a team to look at liquefaction effects in Imperial County and their reconnaissance began on April 6 and finished on April 8. The California Geological Survey also sent a team who spent their first day,

April 8, with the USGS along the northern extent of the Westside Main Canal, and on the subsequent four days followed up on newspaper and verbal accounts of road closures, levee damage, and other effects reported in southern Imperial County.

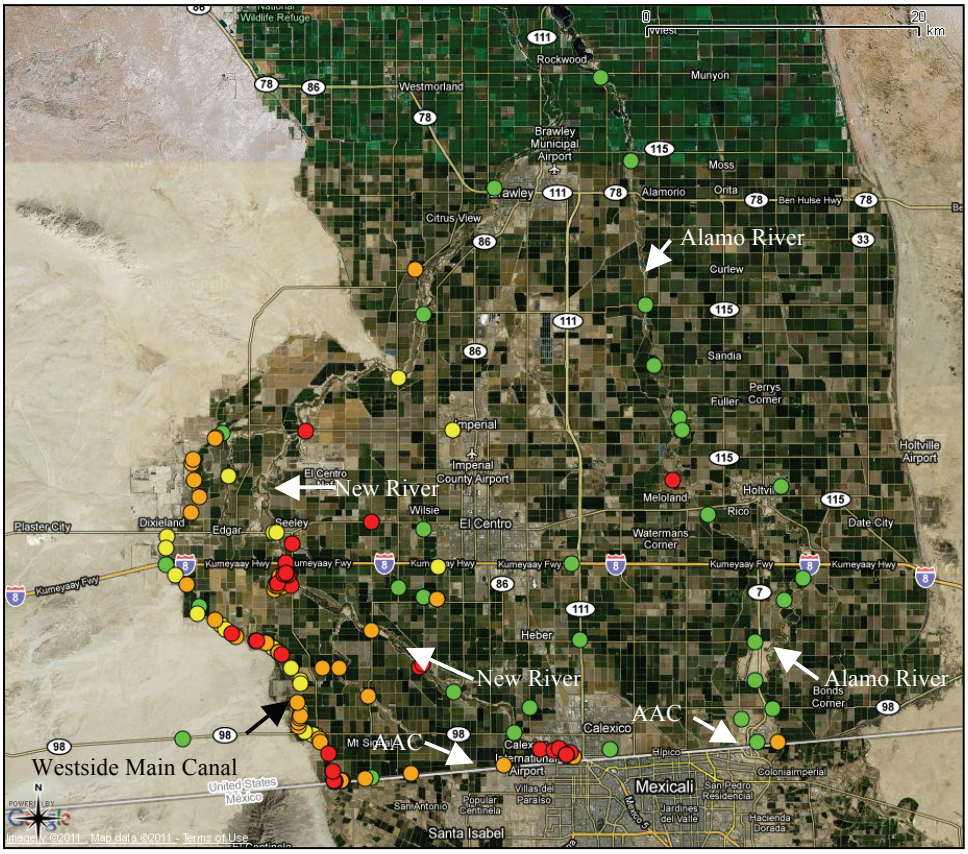

Figure 3. Distribution of sites visited during the liquefaction reconnaissance in Imperial County. Red dots show sites where liquefaction could be confirmed by the presence of sand boils, sand- or silt-filled fissures, or eyewitness accounts. Orange dots indicate sites where the nature of the observed ground deformation was consistent with liquefaction as the primary cause, but no ejected or vented sand was observed. Yellow dots show sites where liquefaction may have contributed but is not required to explain the observed ground deformation. Finally, green dots are sites where no evidence of liquefaction was found. These dots mark other shaking effects, such as slope failures, seiching, evidence of shaking-induced structure displacement, and sites of past liquefaction that did not recur during this event. The Alamo River, New River, All American Canal (AAC), and Westside Main Canal courses are revealed by alignments of dots showing loci of observations. Base image is from Google Maps (2010).

The following sections present the field observations of affected areas north of the international border that were recorded by the three reconnaissance teams. The reconnaissance efforts focused principally on instances if liquefaction and associated effects, but other earthquake effects, such as slope failures, seiching in water bodies, and strong shaking effects on cultural features were also recorded.

Sites visited and described here have been categorized into four groups based upon the predominant infrastructure or facility damaged, the natural feature damaged, or the access road from which the earthquake shaking effect was observed. Each site, often an aggregation of individual GPS waypoints, was given a descriptive name and unique site identifier composed of its group category and relative distance from the seismic source. The categories are roads and bridges (site identification (ID) prefix R); irrigation canals (site ID prefix C); drains and rivers (site ID

prefix D); and major facilities and earthen dams (site ID prefix F). The site identifier is provided in parentheses next to the site name in the text of this report and the corresponding figure captions. The unique site identifier is also used on plate 1, and both the site name and site identifier are provided in the Detailed Sites table (plate 1 and the Detailed Sites table are in separate files). Only sites with easily visible earthquake effects are described below. For more information on sites not described in the report section, the reader is encouraged to review the Detailed Sites table (Microsoft Excel Format).

Roads and Bridges

Brockman Road at Greeson Drain (R02)

The Brockman Road crossing of Greeson Drain consists of a timber bridge supported on timber piles. The plan dimensions of the bridge are approximately 7 m × 8 m. No vented sand was observed at this bridge or the surrounding area. However, lateral spreading of the south bank of the drain (fig. 4), settlement of fill at both approaches, and lateral spreading of the northeast fill shoulder (fig. 5*A*) suggest that liquefaction occurred either below or within the fill. Strong shaking of the bridge structure appears to have split one of the guardrail support posts (fig. 5*A*). The fill settlement was pronounced enough for the authorities to close the bridge to traffic, though it could still be safely crossed at slow speed.

Figure 4. Lateral spread ground cracking on the north bank of Greeson Drain beneath the Brockman Road Bridge (R02). Photo by E. Seyhan, 4/5/10.

Brockman Road at the New River (R05)

The Brockman Road overcrossing of the New River exhibited ground deformation consisting of embankment fill separating from the abutment in the transverse (fig. 6) and longitudinal directions, and longitudinal cracking of the pavement at both approaches (fig. 7). The single-span bridge had plan dimensions of approximately 10 m × 25 m and is supported on concrete piles. On the north side of the bridge, separation between the soil and pile of approximately 8 cm was observed. Along both sides of the road, modest ground cracking, settlements and lateral deformation of 8 cm width and 5 cm height are were observed. Surface evidence of liquefaction in the form of vented sand was not found at this site, though the patterns of ground deformation are consistent with the effects of liquefaction documented at other bridge sites.

A *B*

Figure 5. A, View along east margin of Brockman Road near Greeson Drain (R02) showing fractures and slumping of road fill. Tape in middle ground is 1 m long. Extensional cracking also affected pavement of Brockman Road. B, Strong ground shaking and ground deformation in fill drove the wood guardrail from south to north, causing posts supporting the guardrail to split. Photos by J. Tinsley, 4/7/10.

Figure 6. Approximately 5 cm separation of embankment soil from the concrete abutment at the Brockman Road Bridge over the New River (R05). Photo by E. Seyhan, 4/5/10.

Lyons Road at the New River (R06)

Liquefaction-induced lateral spreading occurred in the New River floodplain at Lyons Road at a distance of roughly 200 m west of the New River bridge crossing and again about 100 m east of the bridge, where the road name changes to Nichols Road. Southwest of the bridge, lateral spreading occurred primarily toward the field on the north side of Lyons Road (fig. 8), though deformation to the east-northeast toward the river was also apparent south of Lyons Road for a distance of at least 100 m. Ground deformation caused horizontal and vertical offsets in road pavement (fig. 9); the road was closed following the earthquake. An irrigation canal adjacent to the north side of Lyons

Figure 7. Ground cracking, settlement, and lateral deformation along the south approach to the Brockman Road Bridge crossing the New River (R05). Photo by E. Seyhan on 4/5/10.

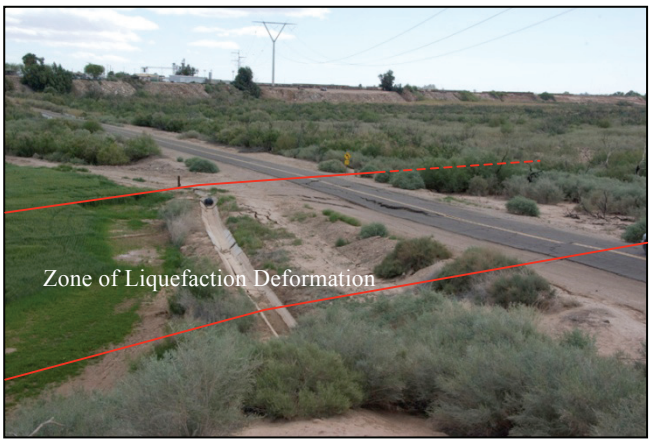

Figure 8. View of damage to Lyons Road and adjacent irrigation canal owing to lateral spreading toward field on left side of image (R06). The approximate area that experienced liquefaction deformation is indicated. The bridge structure over the New River is roughly 200 m farther to the northeast (upper left background in the photo) and suffered no apparent damage. Photo by S. Brandenberg, 4/5/10.

Figure 9. Settlement of Lyons Road pavement and north shoulder owing to lateral spreading within the zone of liquefaction deformation shown in the preceding photo (R06). Photo by S. Brandenberg, 4/5/10.

Figure 10. Effects of lateral spreading on the small irrigation canal adjacent to Lyons Road (R06). Photo by S. Brandenberg, 4/5/10.

Road was also substantially damaged by liquefaction-related deformation (fig. 10). Vented clean fine sand was observed in several places in the southwest corner of an agricultural field north of Lyons Road (fig. 11).

The bridge over the New River is a timber structure with wood piles for support. Unlike most other bridge crossings of the New River where liquefaction was observed, this bridge showed no evidence of shaking distress, and the asphalt surface at the bridge did not contain enlarged cracks.

Roughly 100 m northeast of the bridge, on Nichols Road, less severe settlement was observed, and no vented sand was apparent. A pair of fissures 20 to 30 m apart cross the paved road (fig. 12) and extend into and through the fill embankment on both sides. The upper fissure had about 5 cm vertical separation, down on the downslope side. The lower fissure showed minor compression of the asphalt. Road-parallel fissures formed in the southeast embankment suggesting some insipient lateral spreading on this side. Dense vegetation precluded observations of the surrounding flood plain deposits.

Drew Road at the New River (R07)

Considerable liquefaction-related damage occurred to Drew Road at the bridge crossing the New River. Most of the damage was to the road bed where it was underlain by approach fill. Vented sand was found adjacent to the fill east of the road and north of the river (fig. 13),

Figure 11. Vented sand in the agricultural field immediately north of Lyons Road (R06). Photo by S. Brandenberg, 4/5/10.

Figure 12. Possible liquefaction-related settlement in fill underlying Nichols Road, northeast of the New River (R06). Upper fissure had about 5 cm vertical displacement with extension in the asphalt, whereas the lower fissure had little vertical displacement but showed compression in the asphalt. Road-parallel fissures were observed in the fill embankment to the right of this photo. Photo by T. McCrink, 4/9/10.

Figure 13. Vented sand in the marshy area east of the north approach fill to the Drew Road Bridge (R07). Lateral spreading damage to the road occurred immediately west. Photo by T. McCrink, 4/8/10.

indicating that liquefaction of the soils underlying the fill likely was responsible for the damage. Clear vertical drops in the pavement on both sides of the bridge indicate that liquefaction-related settlement affected 50 m of road north of the bridge and 30 m south of the bridge.

The approach fill on the north side of the bridge spread laterally, opening large road-parallel fissures and grabens (fig. 14). Pre-existing cracks in asphalt were opened up and showed evidence of adjacent asphalt slabs pounding and grinding against each other. Asphalt adjoining the concrete bridge structure on both sides was pushed up and broken into cobble- and gravel-size particles (fig. 15).

Fill at the north bridge abutment dropped at least 10 cm. The bridge piers under the north abutment pushed surrounding soil leaving 10 to 20 cm openings, and the concrete abutment was cracked and spalled (fig. 16). Combined with the battered asphalt at the bridge edges, the soil

Figure 14. Lateral spreading of the north approach fill to the Drew Road Bridge (R07). Vented sand shown in figure 13 is immediately left of this photo. View to the south. Photo by T. McCrink, 4/8/10.

Figure 15. Battered asphalt on the north side of the concrete Drew Road Bridge structure (R07). Similar deformation was found on the south side as well. View to the northeast. Photo by T. McCrink, 4/8/10.

disturbance around the piers suggests significant north-south movement of the bridge structure during the earthquake due to shaking.

Interstate Highway 8 at the New River (R08)

Interstate Highway 8 and a portion of the Drew Road onramp showed extensional cracking in the road fill and pavement where underlain by New River valley sediments near the fill's east margin. California Department of Transportation (CALTRANS) crews were filling and sanding fractures the morning of 4/7/2010, three days after the earthquake (fig. 17). Although liquefaction was not confirmed by the presence of vented sand in the extensional fractures, vented sand was present on the New River floodplain on both sides of the New River channel not far from the location of the deformed highway pavement (figs. 18 and 19). The highway was not closed, although traffic was restricted on the on-ramp while minor repairs and sanding were completed.

Figure 16. View of the concrete pier under the northeast corner of the Drew Road Bridge abutment (R07). Soil pushed away from the pier coupled with the battered asphalt on the road above (fig. 15) suggests that the bridge structure experienced large shaking displacements. Note spalled and cracked concrete in the abutment in the upper right corner of photograph. Photo by T. McCrink, 4/8/10.

A *B*

Figure 17. Extensional fractures across the westbound lanes of Interstate 8 and the Drew Road onramp (R08). *A,* Fractures as they appeared on 4/5/10. Photo by D. Y. Kwak. *B,* Fractures after being patched and sanded on 4/7/10. Photo by J. Tinsley.

Interstate Highway 8 at Sunbeam Lake (R10)

Minor cracking of Interstate Highway 8 fill embankment and the adjacent embankment that forms an access road was observed at the southern end of Sunbeam Lake (fig. 20). The cracks were very small in size, never wider than 2 cm, but they form a "V" shape that opens toward the lake and that suggests they are a result of minor settlement in the fills. There is a presumed culvert running beneath the highway in this area that connects Sunbeam Lake with a small extension of the lake south of the Interstate Highway.

Evan Hewes Highway (S80) at the New River (R13)

No liquefaction effects were observed on the New River Flood Plain where Evan Hewes Highway crosses the New River west of Seeley. In addition, no apparent damage was sustained by

Figure 18. Extensional fractures and fill failure on the north side of Interstate Highway 8 and east bank floodplain of the New River, just north of the extensional fractures shown in figure 17 (R08). All deformation here inferred to be due to liquefaction on the basis of the presence of lateral spread fissures and vented sand on the New River flood plain 50 m or less to the west. Photo by J. Tinsley, 4/7/10.

Figure 19. Lateral spread fissures and vented sand north of Interstate Highway 8 on the east bank of the New River (R08). These liquefaction features were only 50 m or less from the fill failure and pavement fractures shown in the previous figures, and they strongly suggest that liquefaction is responsible for the deformation of the highway. Photo by E. Seyhan, 4/5/10.

the bridge, which is an earth fill over a culvert. However, fill settlements in the upper part of the fills on both sides of the New River, estimated at 25 to 30 cm, required road crews to place asphalt patches on the road by 4/7/10. The east side of this highway experienced a 125-m-long slump or "block glide" with as much as 5 cm vertical separation during the 1968 Borrego Mountain earthquake (Castle and Youd, 1972). A photograph of the reported slump (Castle and Youd, 1972; *their* fig. 113) shows the "headwall scarp" of this failure in the same vicinity as the eastern limit of the zone of settlement, suggesting that the modes of failure from this and the earlier earthquakes may be the same. However, there is too little information from this or the earlier earthquake to distinguish whether the failures are related to sliding (discrete failure surface) or to settlement.

A B

Figure 20. Minor cracks in fill at Interstate Highway 8 at the southern end of Sunbeam Lake (R10). *A,* Southeast-trending crack running obliquely through the Interstate Highway embankment. Photo by T. McCrink, 4/12/10. *B,* View to the west of a southwest-trending crack in access road fill. Person in the background is at the matching southeast-trending crack that forms the V-shaped pattern of cracks that open toward the lake on right. Photo by C. Pridmore, 4/12/10.

Hetzel Road at Salt Creek Drain (R16)

The Hetzel Road Bridge over Salt Creek Drain is a concrete span with concrete abutments. The road was closed at the time it was visited on 4/12/10, though the damage appeared to be minimal. Old cracks in asphalt pavement on both sides of the bridge appeared to have been enlarged as much as 2 cm by shaking (fig. 21). New cracks in asphalt continued into road shoulder and fill materials. Incipient lateral spread cracks on the road shoulders in approach fills were observed but they were generally small (~1 to 2 cm wide; fig. 21*A*), (Note: the term "incipient" is used here to denote cracking with less than about 5 cm cumulative displacement.) No vented sand was observed, but very little of the creek banks could be observed owing to the presence of dense vegetation.

Worthington Road at the New River (R18)

The bridge crossing of Worthington Road over the New River is the farthest north site where liquefaction was confirmed along the New River, and the resulting damage led to road closure. On the east side of the river, light gray sand was found vented on the south side of the bridge approach fill (fig. 22*A*), suggesting the source of the sand is below the fill. On the north side of the fill, at its base, brown sand was vented (fig. 22*B*), suggesting that fill materials, more characteristically brown in color, also were involved in liquefaction. Samples of the light gray vented material were collected and grain size analyses are presented in appendix A (Sample ID IMC–162).

Cracks from lateral spreading were observed on both sides of the west approach fill (fig. 23) but no vented sand was found. The bridge structure recorded movement in response to strong shaking in the form of soil pushed away at the base and sides of the bridge abutments (fig. 24). Additional liquefaction-related features include a series of cracks along and parallel to the river's bank northeast and southwest of the bridge. On the northeast side, the cracks extend as much as100 m north of the bridge and a part of the river's bank slumped into the river with a vertical displacement of as much as 1 m. On the southwest side, river-parallel cracks were found to extend

A *B*

Figure 21. Typical shaking effects at Hetzel Road Bridge over Salt Creek Drain (R16). *A,* Incipient lateral spread cracks in the north side of the approach fill west of the drain (Photo by T. McCrink, 4/12/10). *B,* Pre-existing pavement cracks enlarged by shaking, and new cracks that continue into approach fill (Photo by C. Pridmore, 4/12/10).

A *B*

Figure 22. Sand vented on approach fill on the east side of the Worthington Road Bridge over the New River (R18). *A,* Light gray sand vented on the south side of the east approach fill indicates river sediments beneath the approach fill liquefied, whereas *B,* brown sand vented at the base of the fill on the north side indicates that fill materials liquefied also. Photos by C. Pridmore, 4/8/10.

for about 50 m south of the bridge. Other areas of the river's bank were obscured from view by dense vegetation.

Liquefaction effects were reported for the New River floodplain at Worthington Road for the 1968 Borrego Mountain earthquake. Vented sand and landward slumps at this location were one of the few clear occurrences of liquefaction from that earthquake, and occurred 55 km southeast of the epicenter (Castle and Youd, 1972). Liquefaction was also reported to have severely damaged the approach fill on both sides of the Worthington Road Bridge in the 1987 Superstition

Figure 23. Lateral spreading fissures in approach fill on the northwest side of the Worthington Road Bridge over the New River (R18). Similar fissures were observed on the south side, but no vented sand was found. View is to the west. Photo by T. McCrink, 4/8/10.

Figure 24. Bridge fill pushed away by the Worthington Road Bridge abutment due to strong shaking (R18). Photo by T. McCrink, 4/8/10.

Hills earthquake, resulting in replacement of the bridge (Meehan and others, 1988; Stover and Coffman, 1993).

Forrester Road at the New River (R22)

Observations were made at the Forrester Road crossing of the New River, just north of the intersection with Larsen Road. Cracks in road fill and adjacent alluvium along Larsen Road next to the river indicate some minor movement (2 millimeters (mm)) toward the river free face. No vented sands were found. The driven pile foundation of the Forrester Road Bridge appeared undamaged. Shallow soil slips of loose colluvial material were observed on the steep bluffs south and southeast of the bridge. These soil slides occurred as 5- to 20-m-wide coherent crusts of colluvial material with 10 to 30 cm of displacement at their heads, or linear slip cracks at the interface of the colluvial material and well-cemented soil near bluff tops with 5 to 10 cm of displacement (figure 25).

Keystone Road at the New River (R23)

At the Keystone Road crossing over the New River, no liquefaction features were observed and no road or bridge damage was noted. Some slope effects were observed such as shallow soil slips, small soil-block topples, and minor ridge-top shattering (figs. 26 and 27). Some soil blocks appear to have tilted into an incipient failure position, and they may fail during future rainstorms (fig. 27*A*). A nearly continuous slip of loose, colluvial soil of as much as 5 cm away from the stiff, blocky soil at the bluff top was observed along the slope southeast of the bridge. Nearly all these slope displacements occur or originate at the upper parts of the slopes.

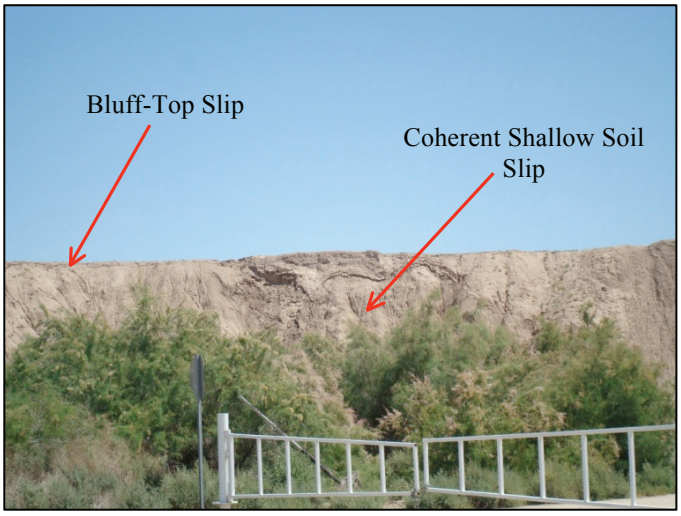

Figure 25. Shallow colluvial soil slips on steep slopes southeast of the Forrester Road Bridge over the New River (R22). Photo by T. McCrink, 4/8/10.

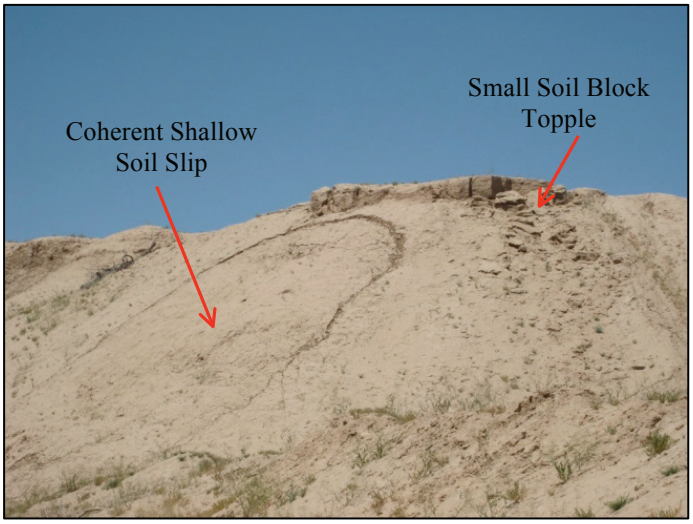

Figure 26. View of the roadcut northwest of the Keystone Road Bridge (R23). A shallow soil slip with 10 to 15 cm displacement is evident on the left side of the photo, and a soil block topple is visible on the upper right. Photo by C. Pridmore, 4/810.

A *B*

Figure 27. Slope effects near the top of the New River bluff at the Keystone Road Bridge (R23). *A*, View of Keystone Road Bridge at the New River with detached mass of colluvial soil in foreground. View to the northeast. *B*, Shattered soil crust on small east-west ridge southwest of the Keystone Road Bridge. Photos by T. McCrink, 4/810.

State Highway 86 (West Main Street) at the New River (R36)

Although the flood plain of the New River experienced extensive liquefaction in the 1979 Imperial Valley earthquake and the bridge structure was so damaged that it had to be replaced, no liquefaction features were observed at this location from this earthquake. Minor riverbank cracking and 1 to 2 cm separation of soil from the bridge piers were the only manifestations of strong shaking (fig. 28).

A *B*

Figure 28. Indications of earthquake shaking at the State Highway 86 Bridge over the New River (R36). *A*, Minor soil cracks on the west bank of the New River beneath the bridge. Photo by J. Tinsley, 4/8/10. *B,* Soil apparently pushed 1 to 2 cm away from bridge pier on the west bank. Photo by T. McCrink, 4/8/10.

Irrigation Canals

Westside Main Canal

The Westside Main Canal extends towards the Salton Sea northward from the western terminus of the All American Canal. A number of lateral canals diverge from the Westside Main Canal and distribute water for irrigation of crops across parts of the Imperial Valley west of the New River. Damage to the Westside Main Canal was evaluated by continuous driving of the canal's levee roads from the All American Canal to Huff Road on the north. It was also observed at Forrester Road, Fites Road (see Cook Drain at Fites Road site in the Drains and Rivers section of this report), and at several locations along West Carter Road south of State Highway 86.

The Westside Main Canal did not fail, but slumps and fissures of variable sizes and extents were common from the All American Canal north to the Fillaree Canal diversion, at the bridge where Westmorland and Boley roads meet. The frequency and intensity of damage generally decreased northward, away from the earthquake epicenter. The Westside Main Canal sustained its most severe liquefaction-related damage south of Interstate 8, between Interstate 8 and the confluence with the All American Canal. North of Interstate 8, and especially north of Evan Hewes Highway (County Highway S80), observed ground failures were mainly limited to bank caving and, in a few locations, to incipient lateral spreads. The latter contained a few millimeters of horizontal displacement, enough to open a few arcuate fractures that defined the failure zone, but not enough displacement to imperil the function of the Westside Main Canal.

The sites described below are presented in order of increasing distance from the seismic source, and smaller canals as well as drains adjacent to the Westside Main Canal are included in this section of the report. Geographic reference points that could be used for locating individual sites along the Westside Main Canal are generally lacking. Therefore, a pair of site reference maps has been prepared to assist the reader (figs. 29 and 50). Secondary canals and drains adjacent to the All American Canal are included here for convenience.

Westside Main Canal and Wormwood Canal at the All American Canal (C01)

Extensive liquefaction and related deformation occurred at the Westside Main Canal and the much smaller Wormwood Canal where they receive water from the western terminus of the All American Canal (fig. 30). Liquefaction-induced lateral spreading is present on both sides of the Westside Main Canal and on both sides of the adjacent Wormwood Canal, with a visibly displaced concrete liner in the Wormwood Canal. Liquefaction was confirmed by sand erupted from extensional fracture sets and at the bases of tilted utility poles, a deformed stream gauging station, and related settlements of embankments (figs. 31 to 35). South of the All American Canal, sand was vented subaqueously in a large puddle (fig. 36). Settlement cracks on the embankment supporting the international border fence bracket a 20-m-wide zone of settlement that coincides with the old trace of the Westside Main Canal, which used to enter the United States from Mexico prior to the construction of the All American Canal.

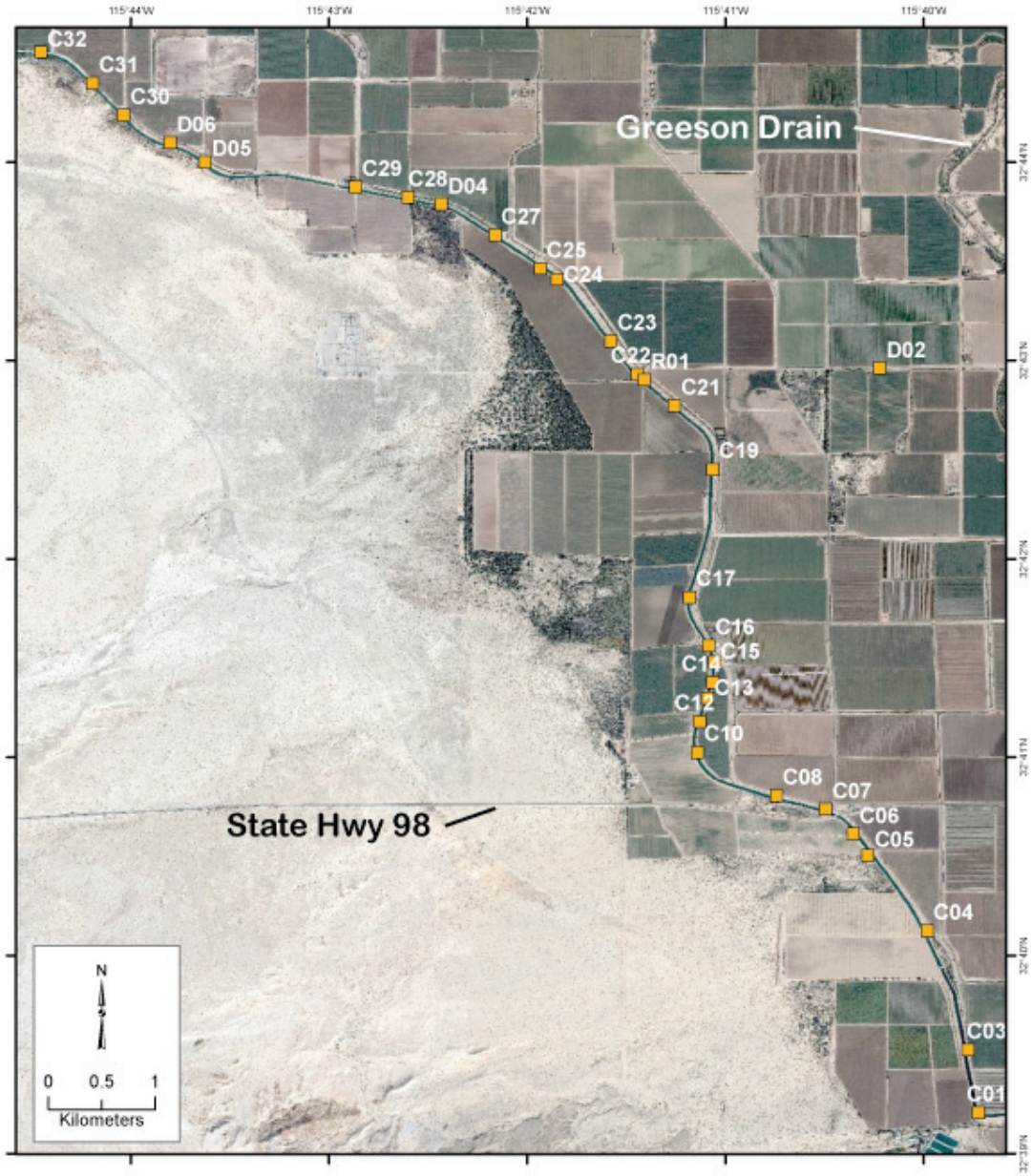

Figure 29. Location of ground failure sites along the southern extent of the Westside Main Canal, from Site C1 in the southeast corner to Site C32 in the northwest. In this reach, the Westside Main Canal skirts the western margin of irrigated land in the southwestern aspect of the Imperial Valley. The principal east-west trending highway in the lower third of this image is State Highway 98 (Yuha Cutoff), and the Greeson Drain is visible in the northeast corner of this image. The letter designation preceding site numbers indicates the structure or facility type at the site: C – irrigation canals; D – drains and rivers; R – roads and bridges; and F – major facilities and earthen dams. National Agricultural Imagery Program (NAIP), 2005, orthophoto base.

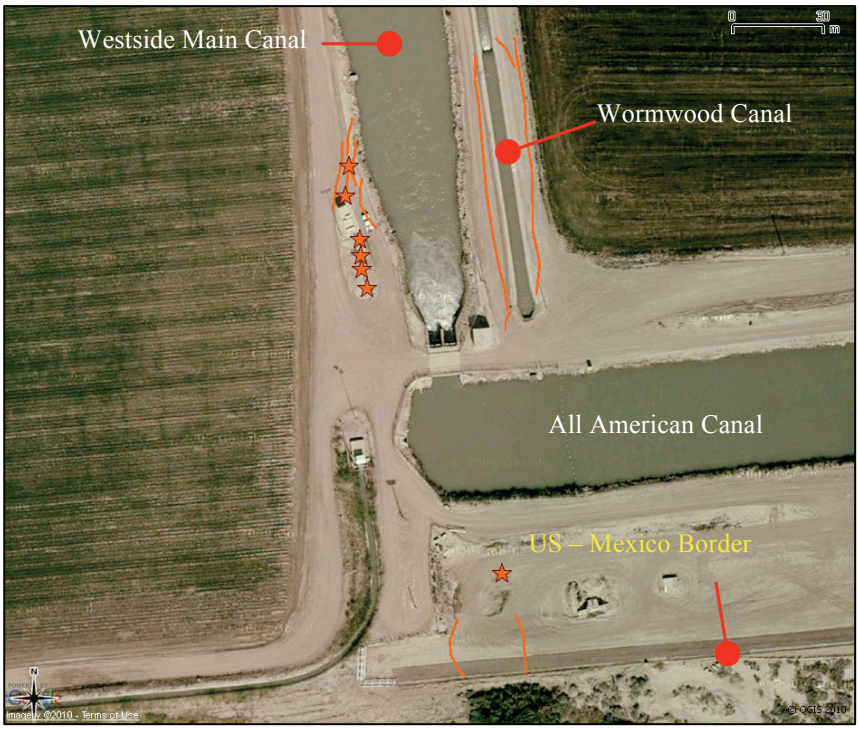

Figure 30. Diagrammatic view of the locations of vented sand (red stars) and related cracks and fissures (red lines) for the western end of the All American Canal and the southern end (start) of the Westside Main Canal (C01). Cracks south of the All American Canal coincide with the old alignment of the Westside Main Canal, and settlement of fill in this old canal appears to have displaced the International Border fence. Base Image is from Google Maps.

Figure 31. Images of Wormwood Canal flowing north from diversion from the All American Canal adjacent to Westside Main Canal (C01). The Westside Main Canal is visible to the west of Wormwood Canal. Lateral spreads on both sides of Wormwood Canal locally deformed the concrete liner, although the canal continued to function. Scarp height indicates about 14 cm of differential settlement. Photos by J. Tinsley, 4/6/10.

Figure 32. View north along west bank of Westside Main Canal, showing utility poles tilted from plumb due to lateral spreading ground failure (C01). Area around base of poles shows light-toned vented sand. Venting of sand in proximity to the poles probably reflects soil-structure interaction that enhanced liquefaction. Photos by J. Tinsley, 4/6/10.

Figure 33. Principal fracture linking two tilted utility poles, showing vented sand with some water still seeping from pressurized strata in subsurface three days after the earthquake (C01). The role of large aftershocks in maintaining elevated pore-fluid pressures is suspected but uncertain. Green plastic scale is 15 cm long. Photo by J.Tinsley, 4/6/10.

Figure 34. Former stage gauge stilling tower tilted from vertical at the Westside Main Canal; associated structures visible to the right of the tower were also tilted from plumb and damaged (C01). No vented materials visible locally. Photo by J. Tinsley, 4/6/10.

Figure 35. Liquefaction-induced extensional fracture near the junction of the Westside Main and All American canals (C01). Exposed pipe or conduit offset 70 mm. Vented sand partly fills fracture underneath the offset pipe. Spreading vector was towards the Westside Main Canal. Photo by J. Tinsley, 4/6/10.

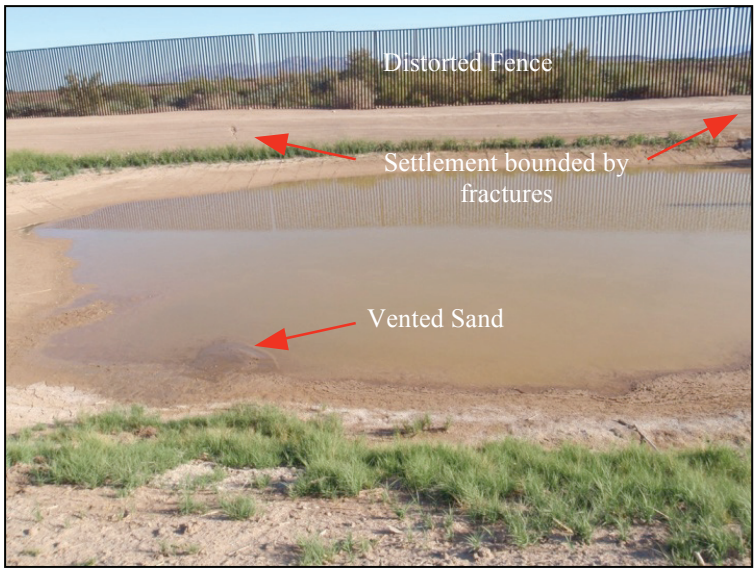

Figure 36. View to south, showing small subaqueous deposit of vented sediment in a puddle of water and, in background, fracture in border fence service road where ground deformation caused a distortion in the border fence (C01). Zone of settlement, as well as the depression forming the puddle, matches the old route of the Westside Main Canal from Mexico. Photo by J. Tinsley, 4/6/10.

Westside Main and Wormwood Canals 600 m North of the All American Canal (C03)

A prominent lateral spread located between the Westside Main Canal and the Wormwood Lateral approximately 600 m north of the start of the Westside Main Canal produced linear scarps extending 50 m parallel to the trends of the two watercourses. Damage to both structures was minimal. The settlement component of ground deformation apparently exceeded lateral displacement at this point (fig. 37).

Figure 37. Lateral spread ground failure in a strip of fill separating the Westside Main Canal (background) from Wormwood Lateral (foreground) (C03). Photo by J. Tinsley, 4/7/10.

Westside Main and Wormwood Canals 550 m North of Anza Road (C04)

On the strip of land between the Westside Main Canal and Wormwood Canal, a lateral spread with a graben at the headscarp extended for 60 m along a trend of N. 27° W. subparallel to the trend of the Westside Main Canal. Displacement was toward the Westside Main Canal and amounted to 3 to 6 cm along the graben. Damage to the canal was not observed and no vented sand was found.

Westside Main Canal West Bank 450 m Southeast of State Highway 98 (C05)

Approximately 450 m south of Highway 98, a part of the Westside Main Canal's western levee collapsed into a void of uncertain origin (fig. 38). An absence of vented sand suggests that the observed ground failure may be ascribed to pre-earthquake piping that caused voids to form beneath the road surface within the levee materials. A nearby well and pump installation also showed evidence of ground settlement.

Westside Main Canal West Bank 250 m Southeast of Highway 98 (C06)

A substantial lateral spread spanned the 19 m width of the west bank levee of the Westside Main Canal and extended into an area of higher ground farther west (fig. 39). These arcuate fractures continue for about 100 m along the channel, and cumulative extensional displacements amounted to about 10 cm at the head of the failure. No vented sand was observed, but liquefaction is a likely cause of the deformation.

Westside Main Canal East Bank 120 m Northwest of State Highway 98 (C07)

A set of extensional fractures subparallel to the east bank of the Westside Main Canal extended about 22 m. Fractures stood open to a depth of 50 cm and horizontal extension amounted to about 9 cm (fig. 40). No vented materials were observed and liquefaction is uncertain. This type of ground failure, which was commonly observed near the Westside Main Canal banks on both sides of the channel, posed no immediate threat to the integrity of the levee.

Figure 38. Collapse of the Westside Main Canal's western access road (C05). Undermining of the road surface probably reflects pre-earthquake piping along transverse subgrade structures or other zone of seepage from the canal. No vented liquefied materials were noted in the area. Photo by J. Tinsley, 4/6/10.

Figure 39. View of extensional fractures at head scarp of lateral spread crossing the embankment in the foreground and including Westside Main Canal's service road to the left (C06). Riparian vegetation is tilted towards the canal owing to lateral spreading. Photo by J. Tinsley, 4/6/10.

Figure 40. Minor extensional fractures parallel to the channel of the Westside Main Canal (C07). No vented materials were observed in association with this ground failure; the failure is likely a result of strong shaking and not liquefaction. Photo by J. Tinsley, 4/7/10.

Westside Main Canal from 250 m to 800 m Northwest of Highway 98 (C08)

A series of shallow slumps in the east and west banks of the Westside Main Canal extended almost continuously for nearly a kilometer north of State Highway 98. Vented soil materials were not observed in association with these bank failures, and the failures likely are due to strong shaking rather than liquefaction. Figure 41 shows a typical example of this type of ground failure.

Westside Main Canal East Bank 2,000 m Northwest of Highway 98 (C14)

A small ground failure, possibly a lateral spread, was observed (fig. 42). Extensional fractures were open to a depth of 94 cm and one single block shows a maximum differential

vertical separation of 16.5 cm near the canal's bank. Neither vented materials nor leakage associated with this ground failure in levee materials was observed. However, the geometry of the failure is consistent with liquefaction.

Westside Main Canal West Bank 380 m South of Kubler Road (C15)

A substantial ground failure, probably a lateral spread, was being repaired by a tracked excavator on the morning of April 7, 2010 (fig. 43). The slumping of the surface of the levee amounted to several tens of centimeters, because vegetation was submerged in the affected reach along the west levee of the Westside Main Canal.

Figure 41. Bank failure probably unrelated to liquefaction in the west bank of Westside Main Canal (C08). This style of failure was observed on both sides of the Westside Main Canal for nearly a kilometer north of State Highway 98. Failures seldom extended more than a meter or two into the levee materials and the bulk of the levees remained undamaged. Photo by J. Tinsley, 4/7/10.

Figure 42. View to north across inferred liquefaction lateral spread in the east bank of the Westside Main Canal (C14). Extensional fractures are open to 95 cm depth and extend across entire width of Westside Main Canal east service road for tens of m. Photo by J. Tinsley, 4/6/10.

Figure 43. Ongoing repairs to the west bank of the Westside Main Canal on 4/7/10 (C15). Tilted and submerged vegetation indicate marked displacement of the levee bank. Photos by J. Tinsley, 4/7/10.

Westside Main Canal East Bank 250 m Northwest of Kubler Road (C17)

A 15-m-long system of fractures extended 6 m from the canal across the east Westside Main Canal levee a short distance north of Kubler Road. The sense of extensional displacement was to the west, towards the canal; magnitudes of horizontal displacement amounted to 30–35 mm, and 15 mm of differential vertical separation characterized the largest fracture. No vented soil materials were observed and the occurrence of liquefaction is uncertain.

Lyons Road Bridge over the Westside Main Canal (R01)

A timber bridge crosses the Westside Main Canal roughly 100 m south of Lyons Road. No damage was observed to the bridge supports, the bridge deck, or to the eastern approach. Differential vertical settlements amounting to 10 to 15 cm were observed in the west approach fill.

Westside Main Canal West Bank 1,170 m Northwest of Lyons Road Bridge (C24)

An arcuate lateral spread developed mainly in the levee fill and disrupted about half the levee road on the west side of the Westside Main Canal (fig. 44). The ground failure was about 40 m long; the most acute ground failure was about 18 m long located in the center of the failed reach of the levee. Differential vertical displacement exceeded 60 cm and horizontal extension towards the free face of the canal channel exceeded 1 m. Soil materials resembling the composition of the levee had welled up in some of the fractures, confirming liquefaction at this site.

Westside Main Canal East and West Banks South of Vogel Road (C25)

A relatively large liquefaction-related ground failure exhibited lateral spreading and settlement across the full width of the west levee of the Westside Main Canal (fig. 45). The zone of failure exceeded 200 m in length. Inward-facing scarplets define the trend of the failure and indicate that the levee most likely sank differentially into a liquefied substrate. Vented liquefied materials were not observed. A small section of levee had recently been repaired on the northeast side of the Westside Main Canal due north of this failure. The nature of the damage of this smaller failure could not be determined.

A *B*

Figure 44. Arcuate lateral spread of levee fill on the west bank of the Westside Main Canal (C24). *A,* View to the south showing a portion of the liquefaction ground failure. Tape measure in center of photo is 1 m long. *B,* View north showing graben developed along system of extensional fractures in liquefaction-induced lateral spread ground failure. Photos by J. Tinsley, 4/7/10.

Figure 45. View to the northwest along the western levee of the Westside Main Canal showing large lateral spread ground failure that spanned the entire width of the levee (C25). The ground failure extended about 200 m along the levee, and the small in-facing scarplets indicate that the levee mass sank differentially into a liquefied substrate. Photo by J. Tinsley, 4/7/10.

Fig Drain East of the Westside Main Canal 700 m Southeast of Liebert Road (D04)

An area at least 100 m long had been extensively regraded by the time it was visited on April 7, 2010. Consistent with previous observations elsewhere along the Westside Main Canal, this ground failure appeared to be a lateral spread east of the east levee of the Westside Main Canal that spread towards the Fig Drain. The Westside Main Canal levees were not damaged at this location.

Westside Main Canal and Fern Canal at Liebert Road (C29)

Several liquefaction-related levee failures of the Westside Main Canal occurred where Liebert Road and the Fern Canal intersect the Westside Main Canal. Roughly 80 m southeast of the Fern Canal diversion, a 12-m-long section of the west levee of the Westside Main Canal settled vertically, creating a 14-cm-high scarp. The scarp trends normal to the Westside Main Canal (fig. 46). Vented sand, silty sand, and sandy silt were observed southwest of the levee, mainly along a south-trending fissure. Samples of the vented material were collected and grain size analyses are presented in appendix A (Sample ID IMC–161).

Another lateral spread was observed approximately 90 m northwest of the previous failure and also on the southwest levee, where a north-south road, possibly an extension of Liebert Road on the north, intersects the Westside Main Canal. However, the canal's function was not impaired as a result of this ground failure because displacements were small and the levee was not fully breached. Vented sand nearby indicates that liquefaction probably caused this ground failure as well.

On the east bank of the Westside Main Canal, a liquefaction-induced lateral spread damaged the diversion controls and liner of the Fern Canal. Repairs by Imperial Irrigation District personnel were in progress on April 7, 2010 (figs. 47 and 48).

Dixie Drain No. 3B along Westside Main Canal 1,240 m Northwest of Liebert Road (D05)

A repaired lateral spread of the eastern-most portion of the east levee of the Westside Main Canal was found at this location. The overall spreading direction was to the east, away from the Westside Main Canal and toward the Dixie Drain. The ground failure apparently affected earth materials mainly east of the east levee, as riprap was undisturbed in its pre-earthquake position along the east bank of the Westside Main Canal.

Dixie Drain No. 3B along Westside Main Canal 1,570 m Northwest of Liebert Road (D06)

A substantial lateral spread developed on the east levee of the Westside Main Canal, including the eastern third of the levee itself, with displacement toward the northeast into Dixie Drain. The Westside Main Canal was not affected by this failure, but the zone of deformation

A *B*

Figure 46. Liquefaction lateral spread and settlement of the southwest bank of the Westside Main Canal (C29). *A,* View to northeast along the western levee of the Westside Main Canal showing the large ground failure that spanned the entire width of the levee. *B,* View to the southeast of fractures and vented sand on the outside of the west levee. Photo by J. Tinsley, on 4/7/10.

A *B*

Figure 47. Lateral spreading fractures on the east levee of Westside Main Canal (C29). *A*, Diversion structure for the Fern Canal was damaged when ground was displaced eastward, away from Westside Main Canal. *B*, Newly poured foundation and wing wall for the Fern Canal outlet from Westside Main Canal. Photos by J. Tinsley, 4/7/10.

A *B*

Figure 48. Repairs to the liquefaction-damaged Fern Canal (C29). *A*, Repair crew adjusts grading equipment to shape walls of the Fern Canal to repair the effects of lateral spread ground failure. *B*, View to the south with Mount Signal (El Centinela) in the distance, showing reshaped canal prior to pouring new concrete walls and bottom. Photos by J. Tinsley, 4/7/10.

extended for about 200 m along its length (fig. 49). Cumulative displacement and settlements were not measured because grading precluded careful inspection of the ground failure. Vented sand was present locally, indicating the apparent role of liquefaction in this ground failure.

Sites along the Westside Main Canal discussed in the text can be located on figure 50 below.

Westside Main Canal East Bank 400 m Northwest of Hyde Road (C33)

The east bank of the Westside Main Canal was observed to bulge west into the flowing channel. The volume of the failure was estimated at to be at least 28 m^3. The failure was about 15 m long and subparallel to the Westside Main Canal, and it appeared to be confined to the fill materials comprising the levee.

A B

Figure 49. Views to the northwest (*A,* and southeast (*B*) of a lateral spread ground failure that developed on the east side of the east levee of the Westside Main Canal (D06). Lateral spread fractures extended for about 200 m. The spreading vector was towards the Dixie Drain No. 3B. Grading equipment has made at least one pass prior to these photos, dumping new material into the zone of extensional cracking and lateral spreading, but the major elements of the lateral spread are still visible. Photo by J. Tinsley, 4/7/10.

Westside Main Canal West Bank 30 m South of Forgetmenot Lateral No. 1 (C34)

A recent, shallow bank failure was observed on the west side of the Westside Main Canal (fig. 51). These sorts of bank failures were extremely common on both sides of the Westside Main Canal throughout the examined reaches. Number, frequency, and persistence of such failures increased towards the south and west in the direction of the seismic source, and they decreased to the north and east as distance to the source zone increased. Bank failures of this type did not generally extend more than a meter or so into bank of the canal, and thus they posed little threat to levee integrity.

Westside Main Canal East Bank 775 m Northwest of Hyde and West Vaughn Roads (C35)

A probable lateral spread was noted at this location, but no vented soil was observed (fig. 52). The volume of the failure was estimated at 35 to 40 m^3. The head scarp of the failure was located about 3 m from the Westside Main Canal water edge and affected a third of the width of the levee.

Westside Main Canal West Bank 875 m Southeast of Interstate Highway 8 (C36)

A series of shallow slumps was noted along a 100-m-long reach of the west levee of the Westside Main Canal (fig. 53). The presence of vegetation rooted in soil blocks below the water level in the canal testifies to the recent vintage of these bank failures.

Westside Main Canal West Bank 2,100 m Northeast of Evan Hewes Highway (C44)

An arcuate fracture set was found traversing the levee roadway on the west side of the Westside Main Canal. The fractures extend from the canal bank across the levee for about 10 m and extend along the trend of the levee for about 28 m (fig. 54). No vented materials were observed and displacements were small. The relation to liquefaction is uncertain but the morphology of the ground failure is compatible with liquefaction.

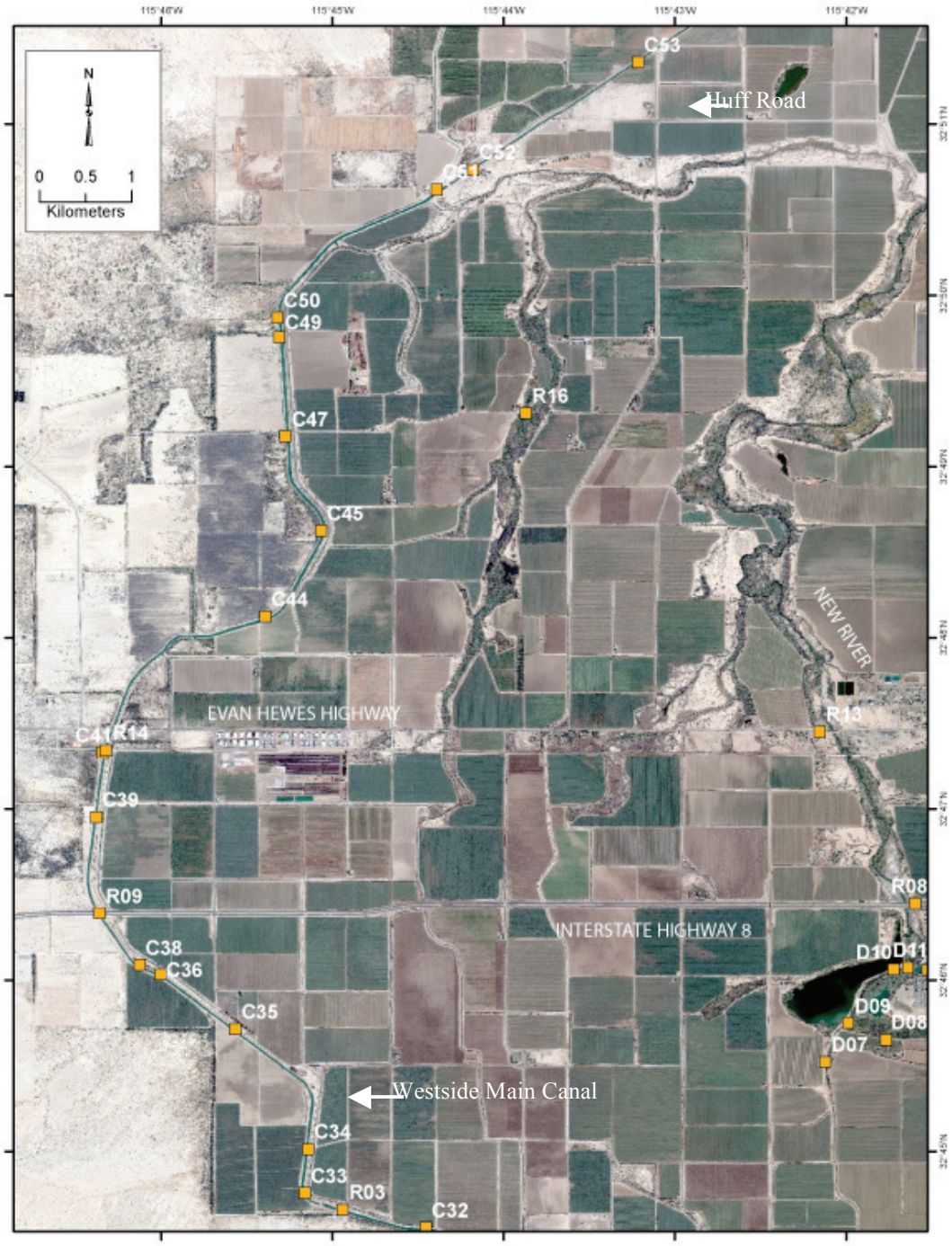

Figure 50. Location of ground failure sites along the central reach of the Westside Main Canal, from site C32 in the south-center to site C53 in the northeast. Interstate Highway 8 and Evan Hewes Highway traverse the southern half of the image and the New River extends along the eastern edge. The letter designation preceding site numbers indicates the structure or facility type at the site: C – irrigation canals; D – drains and rivers; R – roads and bridges; and F – major facilities and earthen dams. National Agriculture Imagery Program (NAIP), 2005, orthophoto base.

Figure 51. View of the west side of Westside Main Canal, showing recent bank failure and slumping of vegetation-bearing soil into the canal (C34). These shallow bank failures were extremely common on both sides of the Westside Main Canal throughout the examined reaches. Photo by J. Tinsley, 4/7/10.

Figure 52. Probable liquefaction-related lateral spread slump into the Westside Main Canal (C35). Soil was being imported on 4/7/10 prior to repairs. Photo by J. Tinsley, 4/7/10.

Westside Main Canal West Bank 2,200 m Southwest of the Bridge at Westmorland Road (C50)

A set of minor fractures penetrates about halfway across the Westside Main Canal levee road. Cumulative extension was small, amounting to about 3 cm on three separate fractures; the extension vector was toward the canal. The zone of failure was about 40 m long and trended parallel to the Westside Main Canal. There were no vented soils observed, but the shape of the fractures is suggestive of liquefaction.

Westside Main Canal at the Fillaree Canal Diversion, South of the Bridge at Boley and Westmorland Roads (C51, R17)

From the Fillaree diversion from the Westside Main Canal and extending at least 250 m south, a 1- to 2-m-wide slump of the Westside Main Canal's west bank was triggered by the earthquake. Extensional fractures toward the canal had cumulative displacements on the order of 30 cm and vertical separations roughly half that (fig. 55). For at least the southwesterly 100 m of this damaged levee, cracks parallel to the canal with a maximum 5 cm vertical or extensional

Figure 53. View to the west showing shallow slumping of the Westside Main Canal wall that dropped vegetation into the canal and oversteepened the canal-side face of the levee (C36). This stretch of slumping extended for 100 m. Photo by J. Tinsley, 4/7/10.

Figure 54. Set of three arcuate fractures across the full width of the levee on the west side of the Westside Main Canal (C44). Displacements amounted to a few millimeters, and the fracture set extended about 28 m along the Westside Main Canal. The last set of fractures is at the toes of the geologist on the left. Although no vented materials were observed, the morphology of the failure is consistent with the type of deformation produced by liquefaction. Photo by C. Pridmore, 4/8/10.

A *B*

Figure 55. Failure of the Westside Main Canal west bank south of the Fillaree diversion structure (C51). *A*, View to northeast; excavator in the background is making repairs. *B*, View to the southwest of the same bank failure. Fractures end where the levee road turns to the right. Vegetation along the canal bank is tilted towards the channel and displaced tens of centimeters. Photos by T. McCrink, 4/8/2010.

offsets extended through the entire levee road, which is approximately 10 to 12 m wide in this area (fig. 56). Vented sand was not observed, but liquefaction is inferred from the nature of the failures. On April 8, 2010, a track-mounted excavator was just beginning to make repairs to the shallow bank failure along this section of levee.

For a 300 m stretch of the Westside Main Canal north of the bridge at Westmorland Road, shallow sloughing of the west bank was observed to be nearly continuous. Beyond that point, similar shallow failures, with volumes in the 1 to 3 m^3 range, were intermittent all the way to Huff Road.

The bridge structure crossing the Westside Main Canal (R17) at this site contained no apparent effects from the earthquake, and it was used to transport heavy equipment to the west bank for the observed repairs.

All American Canal

The All American Canal conveys water 130 km from the Colorado River into the Imperial Valley of California, providing water for more than 200,000 hectares of agriculture and drinking water for at least nine cities; it is one of the largest irrigation canals in the world. The U.S. Bureau of Reclamation began construction on the All American Canal in the 1930s, and it was completed in 1942. The Imperial Irrigation District operates the canal and its distributaries. Runoff from irrigated farmland sustains the New and Alamo Rivers, which drain north to the Salton Sea.

The All American Canal generally performed well during the earthquake, withstanding PGA values apparently in excess of 0.5 g near its southwestern end and about 0.3 g in Calexico. Much of the damage to levees was limited to fractures and lateral spread slumps with cumulative

Figure 56. View to the northeast of fractures running through the outer edge of the Westside Main Canal levee road (C51). Extensional and vertical displacements are one to several centimeters with displacement downward and toward the canal. Photo by C. Pridmore, 4/8/10.

displacements of less than half a meter. Reconnaissance of the All American Canal extended from its western terminus, where it flows into the Westside Main Canal, east to where the All American Canal crosses the Alamo River. For safety reasons, reconnaissance teams were discouraged from travelling on the south side of the All American Canal by the Border Patrol. Early damage reports obtained from the Imperial Irrigation District (S. Gonzalez, IID, 2010, written commun.) indicate that damage to levees occurred as far to the east as the Eastside Main Canal. However, these easternmost sections of the All American Canal were not evaluated for liquefaction-related damage by any of the reconnaissance teams. As before, the sites along the All American Canal discussed below are in order of closest to farthest distance to the surface fault rupture. Secondary canals and drains adjacent to the All American Canal are discussed here for convenience.

All American Canal West of Pullman Road (C02)

Three sets of slump and arcuate extensional fractures deform the north bank of All American Canal along the stretch running roughly 50 to 150 m west of Pullman Road (figs. 57 and 58). Failures were as much as 58 m long and open fractures were plumbed to depths ranging from 0.5 to about 1.35 m. Differential settlements were as much as 8.5 cm, and total extension across the fractures ranged from 5 to 20 cm. Maximum slump widths generally extend about half to two-thirds of the width of embankment (3 to 5 m). No vented liquefied materials were observed, but liquefaction is deemed likely owing to the depth of open fractures and the presence of inward-facing scarplets showing differential settlement of the embankment's crest.

All American Canal 370 m West of Brockman Road (C09)

A small slump was observed on the inside edge of north embankment of All American Canal west of Brockman Road. The slump is 23 m long and had 8- to 15-cm-wide extensional

cracks (fig. 59). Active seepage was present on the outside edge of the levee north of this slump feature, and water-softened materials would not support the weight of a person. Parts of a small irrigation ditch north and east of this location along the All American Canal (C11) had damaged concrete liner, showing evidence of strong shaking.

Figure 57. View looking west across the westernmost set of arcuate extensional fractures that deformed the north bank of All American Canal near Pullman Road (C02). This failure is 58 m long and open fractures were plumbed to depths of about 135 cm. Differential settlement is about 85 mm and total extension across apparent lateral spread is greater than 12 cm. No vented materials noted. Building in the distance marks the end of the All American Canal and the beginning of the Westside Main Canal. Photo by J. Tinsley, 4/6/10.

Figure 58. Wide-angle perspective image showing an incipient extensional failure that extends nearly across the entire width of the north embankment of the All American Canal near Pullman Road (C02). Total length of southward-extensional deformation exceeds 30 m. Liquefaction unconfirmed as no liquefied materials were vented. In-facing scarps indicate differential settlement involving the highest parts of the earthen levee. This pattern of deformation is consistent with liquefaction. Photo by J. Tinsley, 4/6/10.

All American Canal at the Woodbine Lateral 2 (C18)

Arcuate slump–lateral spread features formed on both sides of the Woodbine Lateral 2 diversion structure. These slumped areas were 15 to 20 m wide and extended through the full 10 m width of the levee road (fig. 60). No vented sand was observed, but the type of deformation here is consistent with liquefaction. A track-mounted excavator was observed repairing the levee roughly 300 m to the east of the Woodbine Lateral, suggesting that similar slumps may have occurred along much of this section (fig. 61).

All American Canal at the Greeson Drain (C26)

All American Canal levee repairs were under way on the afternoon of April 5, 2010, one day after the earthquake, but the nature of the damage was not determined. Yellow caution tape

A *B*

Figure 59. *A*, Extensional cracking and incipient slumping of the north bank of the All American Canal (C09). Slump is 23 m long with 8 to 15 cm extension. *B*, Active seep on north side of the north embankment, opposite the seemingly minor slump shown in *A*,. Photos by J. Tinsley, 4/6/10.

A *B*

Figure 60. View to the west along the All American Canal showing arcuate fractures and incipient slumping on both sides of the Woodbine Lateral 2 diversion structure (C18). *A*, On the west side, concentric fractures extend through the full width of the levee road. *B*, Fractures on the east side extend right to the outlet structure and also form a concentric pattern deep into the levee. Photos by D.Y. Kwak, 4/5/10.

along the canal edge suggested more slumping into the canal, but heavy equipment was working mostly on the north side of the levee indicating that more damage occurred there (fig. 62).

Wistaria Canal at the All American Canal (C37)

A probable liquefaction lateral spread occurred along the west bank of the Wistaria Canal just north of its outlet from the All American Canal (fig. 63). The deformation extends along the canal for approximately 70 m, and cumulative lateral displacements were on the order of 1 m. Concrete liner was broken and displaced on both sides of the canal. No vented sand was observed.

All American Canal at the Alamo River (C55, D14)

A concrete structure, approximately 125 m long carries the All American Canal over the Alamo River. Incorporated into this structure are a weir and flood gates, an outlet to the Alamo

A *B*

Figure 61. All American Canal repairs east of the Woodbine Lateral 2 (C18). *A*, View to the east along the All American Canal; excavator repairing bank slump in north levee. *B*, View to the west showing recent repairs to levee and access road along the All American Canal. The tree in the upper center of the photo marks the location of the slumps shown in fig. 60. Photos by J. Tinsley, 4/6/10.

A *B*

Figure 62. Levee repairs on the All American Canal east of the Greeson Drain outlet structure (C26). *A*, Track-hoe repairing the outer edge of the north levee. Photo by S. Brandenberg, 4/5/10. *B*, Bulldozer releveling the top of the levee. Photo by D.Y. Kwak, 4/5/10.

River, and a rotating conveyor bridge over the canal. Lateral spreading of the northern All American Canal levee toward the canal occurred both east and west of this structure (fig. 64). On the west side, a set of at least five fissures extended 5 m into the levee road and had a measured cumulative 20 cm of horizontal offset (fig. 65*A*). Although not measured, similar displacements of the All American levee were observed on the east side of the structure (fig. 65*B*). Similar cracking occurred in the 1979 Imperial Valley earthquake (Youd and Wieczorek, 1982*, their* fig. 171) and roughly 150 m of cracks were reported here resulting from the 1987 Superstition Hills earthquake (Finch, 1988*, his* photo 7). Although no sand was vented in this area, the observed deformation is consistent with liquefaction.

A *B*

Figure 63. Lateral spread of the west bank of the Wistaria Canal near its origin at the All American Canal (C37). *A*, Lateral spread damage to the west bank. Photo by D.Y. Kwak, 4/5/10. *B*, Damage to the east bank liner. Photo by W. Lopez, 4/5/10.

Figure 64. Diagrammatic sketch of cracks and fissures observed on the north side of the All American Canal where it crosses the Alamo River (C55). The Alamo River flows to the north beneath the canal. Base Image is from Google Maps.

Cracks with a few centimeters of horizontal displacement were found on both sides of the Alamo River and likely represent incipient lateral spreading (fig. 66). Liquefaction here is possible but not required to have formed these cracks.

Eucalyptus Canal (C40, C48)

The Eucalyptus Canal was the only irrigation canal that exhibited clear evidence of water seiching over the canal levee. This evidence was observed in two places, the first along a 150 m length north of McCabe Road (fig. 67). Surface soils on the west levee clearly showed the effects of water flow, and a large puddle of water was still on the adjacent Nichols Road one week after the earthquake.

Similar water loss along the Eucalyptus Canal was also noted along Nichols Road to the north, just south of Evan Hewes Highway. A resident stated that flooding during the earthquake

A *B*

Figure 65. Lateral spread cracks on the north side of the All American Canal at the Alamo River crossing (C55). *A*, View to the east of cracks west of the canal crossing; rotating conveyor bridge and flood gates are visible in the background. *B*, Cracks on the east side of the Alamo River; view to the east. Photos by E. Seyhan, 4/5/10.

A *B*

Figure 66. Small displacement extensional cracks on the *A*, west side and *B*, east side of the Alamo River immediately north of the All American Canal (D14). Photos by: *A*, T. McCrink, 4/9/10; *B*, E. Seyhan, 4/5/10.

resulted in closure of the road, but no remaining water was visible one week after the earthquake. However, the road closure probably helped preserve the evidence of seiching, in the form of soil erosion on the west levee bank and deposition of soil with flow structures on Nichols Road (fig. 68).

Central Main Canal (C42, C46)

Several slumps of different size were encountered along the Central Main Canal, north of McCabe Road and south of Interstate Highway 8. A 50-m-wide zone of lateral spread cracks extends north from a weir structure 80 m north of McCabe Road, and the northernmost 20 m portion consists of an arcuate slump feature with a 75 cm vertical offset (fig. 69). An accumulation of concrete rubble in the canal adjacent to this area of larger offset suggests that this area has been

Figure 67. View to the southwest along Nichols Road showing ponded water in a low lying area along Nichols Road (C40). This area is located approximately 150 m north of McCabe Road, which is marked by the trees in the background. Soils on the outer levee side that have not been disturbed by postearthquake traffic show erosion caused by water flow. Photo by C. Pridmore, 4/11/10.

A *B*

Figure 68. Area of seiching from the Eucalyptus Canal along Nichols Road south of Evan Hewes Highway (C48). *A*, View to the north of the Eucalyptus Canal and Nichols Road. Water flowed over the canal levee and across Nichols Road resulting in the temporary closure of the road. *B*, Pen is aligned parallel to water flow direction across Nichols Road pavement. Photos by C. Pridmore, 4/11/10.

a problem in the past. Some smaller cracks at the canal edge were observed on the east bank south of the weir. No vented sand was found in this area. A seismic recording station at the McCabe School, roughly 200 m south of this site, recorded a PGA of 0.588 during the El Mayor–Cucapah earthquake.

Slumping of the outer 2 to 3 m of the west bank of the Central Main Canal also occurred south of another weir structure, 110 m south of Interstate Highway 8. The slumping extends for about 25 m south of the weir, and vertical offsets ranged from 10 to 40 cm (fig. 70). A fresh asphalt

A *B*

Figure 69. Slumping on east side of Austin Road just north of McCabe Road, near McCabe School. *A*, Large crack on shoulder of road that was part of fractured area more than 40 m wide (C42) and extended approximately 15 m back from canal. *B*, The slump had a maximum measured vertical displacement of 75 cm. No surface liquefaction features such as vented sand were observed. Photos by C. Pridmore, 4/11/10.

A *B*

Figure 70. Shallow slumping along Austin Road adjacent to the Central Main Canal, just south of Interstate Highway 8 (C46). *A,* View to the north toward the weir and Interstate Highway 8 showing slumping of the outer 2 m of the canal bank. *B,* View to the south at a slump just upstream of the weir showing 30 to 40 cm of vertical displacement. Photos by: *A,* C. Pridmore, 4/11/10; *B*, T. McCrink, 4/11/10.

patch and regrading of the shoulder of Austin Road suggests that deformation may have extended farther back from the Central Main Canal in this area. However, no evidence of vented sand was found in this area.

Rosita Canal North of Bell and Alamo Roads (C56, R28)

The most distant occurrence of liquefaction found for this earthquake was west of the town of Holtville along the Rosita Canal at a distance of 38 km from the fault rupture and 60 km from the epicenter. Liquefaction occurred on both sides of the canal for a distance of 800 m just north of the intersection of East Alamo and Bell roads (fig. 71). At the southeastern end of the damaged area, lateral spreading on both sides and towards the canal was observed despite recent grading of the canal levees. On the south side of the canal, between the canal and East Alamo Road, a graben that ranged from 1 to 2 m wide formed 10 to 15 m away from the canal bank. Evidence of vented sand was found at the base of a telephone/power pole in this same area.

Immediately northeast of the canal, a series of arcuate lateral spread cracks, some filled with vented sand, traverses the front yard of a residence that fronts onto the levee road (fig. 72). Vented sand was observed on both sides of the cracks, but the levee road here was also recently graded, limiting observations of deformation. A continuous line of sand boils was observed in an agricultural field on the west side of the Rosita Canal from East Alamo Road north 500 m to the end of the field (fig. 73). The sand boils did not continue into the next field to the north. These sand boils were as much as 1 m in diameter, and some were found to be wet on April 11, 2010, suggesting either aftershock reactivation or continued seepage from the canal (fig. 74).

Extensive levee repairs were underway on the east side of Rosita Canal on the morning of April 11, 2010, and access was not possible. Repairs were completed by the afternoon when access was gained. The repairs included the import of fill by several large dump trucks, leveling of the levee top, and tamping of the outboard side of the levee with the bucket of a large track-mounted excavator. The need to import fill indicates that the levee top settled by a significant amount in this area. In the small field on the east side of the canal one large and a few small sand boils were

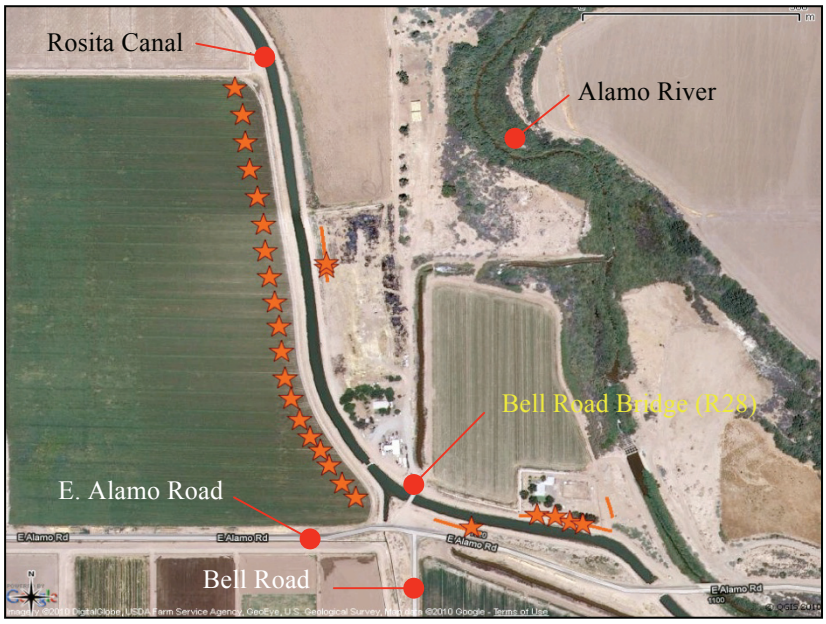

Figure 71. Diagrammatic sketch showing liquefaction features along the Rosita Canal west of Holtville. Lines represent approximate locations of cracks and fissures, and star symbols represent approximate sand boil locations (C56, R28). Base image is from Google maps.

Figure 72. An arcuate lateral spreading crack running through a fenced yard on the north side of the Rosita Canal, northeast of the intersection of East Alamo and Bell roads (C56). Vented sand was found in several areas on both sides and filled some parts of the crack. The levee road, just to the right of the picture, had recently been graded, obliterating any liquefaction features that may have existed. View to the east. Photo by T. McCrink, 4/11/10.

Figure 73. Continuous string of sand boils in an agricultural field west of the Rosita Canal (C56). View to the southeast. Photo by C. Pridmore, 4/11/10.

observed (fig. 75). The large sand boil had an unusually large crater that was 1 m long, 20 cm wide, and 40 cm deep. The sand boils formed along a linear fissure about 40 m east of and parallel to the canal. Another fissure in the field, 30 to 35 m east of the canal and north of that just described, showed evidence of water seepage with little or no vented sediment (fig. 76). Because the focus of the levee repairs was adjacent to this fissure, it appears that liquefaction may have damaged the levee and allowed considerable seepage onto the field. Repairs by compaction with

Figure 74. A pair of sand boils on the west side of the Rosita Canal that were wet 7 days after the earthquake, suggesting reactivation by aftershocks or subsurface conditions enabling prolonged seepage (C56). Photo by T. McCrink, 4/11/10.

Figure 75. Large sand boil that formed along a fissure on the east side of the Rosita Canal (C56). The sand boil has an unusually large crater and the concentric cracks suggest subsequent caving. View to the south; the Rosita Canal is to the right of the picture. Photo by C. Pridmore, 4/11/10.

Figure 76. Evidence of excessive seepage from the east side of the Rosita Canal (C56). The fissure shown is slightly closer to the levee than the fissure related to the sand boils shown in figure 75. View to the north. Photo by T. McCrink, 4/11/10.

the excavator bucket, a common approach observed during this reconnaissance, may have alleviated the immediate seepage problem but are unlikely to prevent liquefaction damage from future earthquakes.

Liquefaction was not reported at this location from the 1979 Imperial Valley earthquake, though liquefaction was suspected in slumps into drains at Zenos Road, 1.2 km southeast and slumps east of the Worthington Road Bridge over the Alamo River, 2.8 km northeast (Youd and Wieczorek, 1982). The occurrence of extensive liquefaction here from this more distant earthquake suggests that pre-earthquake seepage from the Rosita Canal in this area may have created liquefaction-susceptible conditions.

Drains and Rivers

Greeson Drain at Lyons Road (D03)

Settlement and lateral spread deformation was observed in fill and natural deposits in Greeson Drain south of Lyons Road. Lyons Road fill at the west edge of the drain also appears to have experienced settlement in line with settled fill (fig. 77). Most fractures were observed in access road fills south of Lyons Road and west of the drain. These fills range in thickness from 1 to 2 m and contain arcuate cracks with as much as 30 cm vertical separations and extension on the order of 10 cm (fig. 78). The edge of the west access road along the drain had a linear extensional separation that was followed for a distance in excess of 300 m. The separations were as much as 50 cm wide. Some portions of this dirt access road showed the development of paired fissures with down-dropped graben between them. No vented sand was observed but liquefaction is inferred from the morphology and extent of the failures.

This location was visited because of a verbal report by the land owner north of Lyons Road and west of Greeson Drain that described extensive ground cracking at the eastern edge of his fields adjacent to the drain. By the time the area was visited on April 9, 2010, the bottom and slopes of Greeson Drain, as well as the upper edges of the agricultural fields, had been extensively and recently regraded, and the origin of the reported failures could not be determined.

Figure 77. View looking northeast across Lyons Road and down Greeson Drain (D03). The culvert under Lyons Road is located to the right of this photo but the settlement in fill in the foreground appears to continue beneath Lyons Road. North of Lyons Road the drain bottom, slopes, and upper edges have all recently been regraded. Photo by C. Pridmore, 4/9/10.

Figure 78. View to the east across Greeson Drain at liquefaction lateral spread fissures in the access road fill prism (D03). The full width of the road fill settled and the northern two-thirds spread to the north. Photo by C. Pridmore, 4/9/10.

Fig Drain South of Fig Lagoon (D07)

Access to the west side of Fig Drain was partially blocked by numerous soil block falls onto the dirt road, roughly 500 to 600 m south of where the drain enters the New River (fig. 79). These talus cones of blocky soil could be observed on the road for several hundred meters farther to the south. On the east side of the drain in the same area, a 20- to 30-m-wide slump dropped the outer 2 m of the dirt road into the drain. It could not be determined if liquefaction of the saturated soil along the edge of the drain was involved in this slump, as dense vegetation obscured any view of the drain channel or its banks.

A B

Figure 79. Access roads along Fig Drain, south of Fig Lagoon (D07). *A,* Blocky soil topple/fall on the west side of Fig Drain. Several more talus cones of material can be seen in the distance. *B,* Slump of the outer edge of the dirt road on the east side of Fig Drain. Both photos looking south. Photo *A,* by C. Pridmore, and photo *B* by Tim McCrink; 4/10/10.

Fig Lagoon at the New River (D10)

The impact of earthquake shaking at Fig Lagoon emerges as one of the more remarkable case histories encountered in this investigation. Fig Lagoon is a roughly 37 hectare (92 acre) man-made body of water lying south of Interstate Highway 8 and west of Drew Road (fig. 80). It lies in the Holocene floodplain of the New River and was made by the construction of a levee on the west side of the active river channel. A concrete outflow control structure was built near the very northern end of the lagoon. The New River flood plain in this area is incised into older Holocene and Pleistocene alluvial deposits that form uplands on either side of the New River and Fig Lagoon.

The Fig Lagoon area was first visited by the USGS team on 4/7/10. Some grading had been done towards the south end of the impounding levee, but numerous lateral spreads, occurrences of differential subsidence and abundant vented sand indicated that liquefaction of underlying New River deposits was prevalent. Farther north, liquefaction-induced lateral spreads resulted in subsidence and nearly foundered the impounding levee (fig. 81). An outwash channel had developed there, indicating substantial amounts of water had decanted from the lake by way of the channel into the New River and onto the adjacent floodplain (fig. 82). Eyewitness accounts of the appearance of widespread floodwaters on the floodplain following the earthquake were substantiated on April 7, 2010, by the presence of standing water on the floodplain between the New River and the Fig Lagoon levee, downvalley from the liquefaction-induced outflow channel (fig. 83). Evidence of liquefaction continued to be widespread toward the north end of the levee, involving chiefly the alluvial materials underlying the levee, with consequent lateral spread failures induced into the overlying levee itself (fig. 84).

The water level of Fig Lagoon was noticeably lower than recent levels, amounting to as much as a 0.5 m drop, as indicated by freshly exposed lake-bottom sediment, emergent vegetation, and algae-covered riprap (fig. 85). While it is clear that much water was lost over the levee breach (see fig. 83), the outflow structure was observed to allow water to leave the lagoon on 4/7/10 and again on 4/10/10, indicating that some of the drop in water level is due to the agency responsible

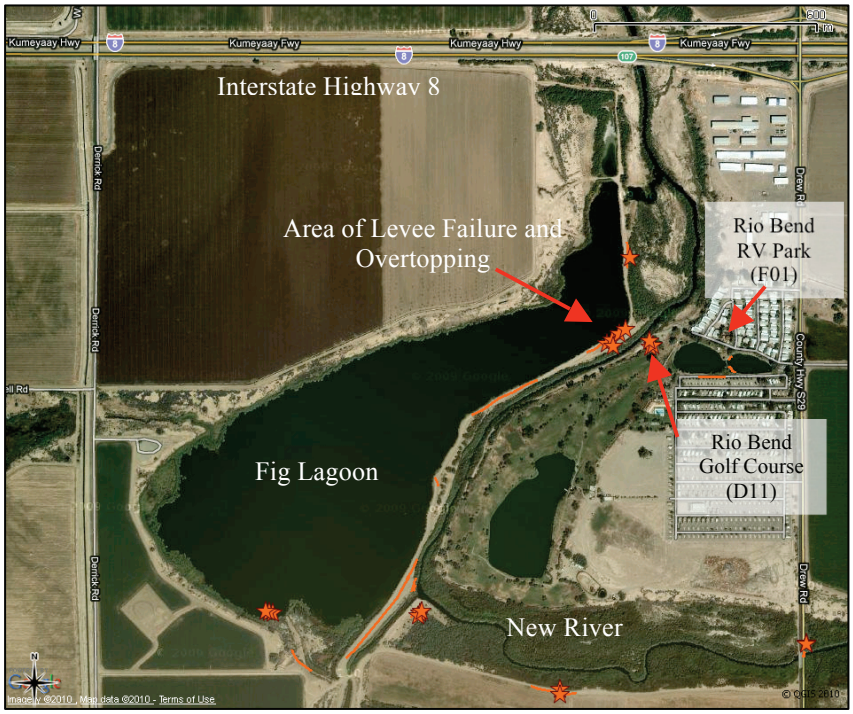

Figure 80. Diagrammatic sketch of liquefaction-related features in the vicinity of Fig Lagoon (D10). Red lines represent lateral spread cracks and red stars represent areas of vented sand. Fig Lagoon lies south of Interstate Highway 8, west of Drew Road, and east of Derrick Road. Also shown are the Rio Bend RV Park and Rio Bend Golf Course sites, which will be discussed in under site entries F01 and D11 respectively. Base image is from Google Maps.

A *B*

Figure 81. Lateral spread–slump failure of the levee between Fig Lagoon and the New River (D10). *A,* View to the northeast along the levee impounding Fig Lagoon, showing liquefaction lateral spread cracks and the large slump that allowed a breach in the levee, overtopped by seiche wave activity. Lake is to the left of riparian vegetation in left foreground of image. *B*, View to the southwest showing the slump and breach in the Fig Lagoon levee. Fig Lake is visible through the vegetation on the right of the image. Standing water is about at the level of Fig Lake. After the earthquake Fig Lake drained near here through an overflow channel that was eroded by escaping lake water. Photos by J. Tinsley, 4/7/10.

A *B*

Figure 82. Depositional and erosional features resulting from seiche wave overtopping of Fig Lagoon levee (D10). *A,* Sand deposition and flow features on the Fig Lagoon levee as a result of overtopping by seiche waves. Water flow came toward the photographer. Lateral spread slump is in the middle background; Fig Lagoon is beyond riparian vegetation on the outer edge of the slump. Photo by T. McCrink, 4/10/10. *B*, Outwash channel eroded into the Fig Lagoon levee adjacent to the New River. Lateral spread slump shown in figure 80 is immediately left of this photo, and the New River is immediately to the right. Photo by J. Tinsley, 4/7/10.

Figure 83. View to north and west from the upland east of the New River channel, showing flooding of the New River floodplain between Fig Lagoon, upper left, and the New River, middle right (D10). Photo by J. Tinsley, 4/7/10.

for the lagoon, likely the Imperial Irrigation District, purposely lowering the lagoon level for safety reasons.

A subsequent visit to the Fig Lagoon area was conducted by the California Geological Survey team on 4/10/10. By that date almost all of the levee system had been regraded; the main

A *B*

Figure 84. Zone of liquefaction-triggered ground failure in Fig Lagoon levee 175 m north of the slump and overflow channel depicted in preceding photos (D10). *A,* Scarps in the levee indicate that differential subsidence into a liquefied substrate probably occurred. *B*, Sand boil deposits presently underwater atop late Holocene floodplain deposits of New River at Fig Lagoon. Preservation of vented materials is morphologically excellent, indicating that a subaqueous eruption is probable. Photos by J. Tinsley, 4/7/10.

A *B*

Figure 85. Indications of significant lowering of the Fig Lagoon water level (D10). *A,* Outfall area at the north end of Fig Lagoon. Algae-covered concrete riprap, emergent vegetation and exposed sediment indicate recent lowering of the lake level. *B*, View from uplands at the south end of Fig Lagoon showing recently emergent lake bottom sediment locally covered with reddish brown vented sand. Photos by J. Tinsley, 4/7/10.

exception was the large slump that caused the levee breach. Aftershock-driven liquefaction on the levee had already produced vented sand on some portions of the regraded levee (fig. 86).

On the basis of observations made around Fig Lagoon, the following events are inferred to have taken place:

1. Earthquake shaking triggered liquefaction in late Holocene alluvium of the New River beneath the levee impounding Fig Lagoon, and locally within the fill materials themselves. Lateral spreading and subsidence of the levee occurred in several places, lowering the levee crest nearly to the level of the water in Fig Lagoon.
2. Seiche wave activity then developed in Fig Lagoon, and the surging resulted in one or more episodes of water sloshing from within the lake and overtopping the levee where it

Figure 86. Vented sand (bottom center) on a recently regraded levee next to Fig Lagoon, indicating that liquefaction of saturated soils continued to occur during aftershocks (D10). Fig Lagoon lies to the right of the vegetation in the upper right. Wet area between graded material in the foreground and vehicle in the background is where lateral spreading and overtopping of lake water occurred (figs. 80 and 81). Photo by C. Pridmore, 4/10/10.

had been damaged by liquefaction-triggered permanent ground deformation. Seiche wave activity is indicated to have been responsible for the overtopping, because the levee would have washed out completely had liquefaction lowered the levee crest below the lake level.

3. The escaping water eroded a shallow, wide channel into the levee, thus forming the well-preserved prominent outwash channel. It could not be determined whether other outwash-related features were obliterated by the locally extensive grading at the southern end of the Fig Lagoon levee system prior to the first visit on 4/7/10.
4. Liquefaction triggered by aftershocks continued for almost a week after the earthquake mainshock.

New River at the Rio Bend Golf Course (D11)

Liquefaction lateral spreading was found on the north side of the golf course adjacent to the New River, across the river southeast of the main levee breach between Fig Lagoon and the New River (see fig. 80). This arcuate spread displaced the ground about 15 cm horizontally to the northwest, toward the active channel of the New River, and included both fill and recent alluvium of the New River. Vented sand, still wet three days after the earthquake, was found near the upper parts of this spread (fig. 87).

Rice Drain No. 3 North of Evan Hewes Highway (D12)

A large liquefaction lateral spread occurred at the southwest corner of an agricultural field located immediately north of Evan Hewes Highway, halfway between the towns of Seeley and El Centro. The lateral spread moved to the west toward the Rice No. 3 drain (fig. 88). The affected area is roughly 80 to 100 m along the Rice Drain, and extends 90 m to the east of Rice Drain.

Figure 87. Liquefaction lateral spread west of the Rio Bend RV Park (D11). Golf course on the left and New River active channel is at the right immediately beyond the line of riparian vegetation. A horizontal extension of about 15 cm was measured. Wet vented sand, dark brown in the photo, was observed here, 3 days after the mainshock. Photo by J. Tinsley, 4/7/10.

Repairs to the lateral spread were underway at the time of the visit (April 9, 2010) and were concentrated on the east bank of the Rice Drain (fig. 89). According to the owner of the field, the west-facing bank of the drain was transported across the drain, depositing salt cedar bushes on the opposite bank. The road on the east bank was severely disrupted by open fissures reported to have been as much as 1 m wide and 30 cm deep prior to the start of repairs (fig. 90). The operator of the

Figure 88. Diagrammatic sketch of liqufaction-related features north of Evan Hewes Highway and east of Rice Drain No. 3 (D12). Lines represent approximate location of cracks and fissures, and star symbols indicate approximate location of sand boils. Base image is from Google Maps; Google label for Forrester Road appears to be in error.

Figure 89. Panoramic view of the lateral spread at Evan Hewes Highway (on the right along the line of telephone poles) and Rice Drain No. 3 (forground) (D12). Repairs underway on the left consist of excavation and replacement of the levee materials. Photos by T. McCrink, 4/9/10.

sheepsfoot roller working on the repair reported that when he turned on the roller's vibrator, water squirted out of the ground and his roller sank to a depth that required a bulldozer to pull it out.

The eastern portion of the lateral spread manifested as a series of arcuate cracks and several sand boils (fig. 91). The sand boils were generally not associated with the fissures, but vented from within soil blocks between them. However, all cracks wide enough to see into were filled to various depths with liquefied silty sand. The fissures showed extensional movement from a few mm to 30 cm wide and a vertical displacement as much as 20 cm.

Discussions with the land owner revealed that clay tile drains that are typically installed in most agricultural fields in the area were not installed in the westernmost 150 m of this field. These drains are usually placed at depths of 2 to 3 m at regular intervals. It may be that the absence of these drains contributed to liquefaction at this location by enabling shallow groundwater to persist after irrigation.

Figure 90. View looking north at the lateral spread into the Rice No. 3 Drain (D12). Owner of the agricultural field reported that the salt cedar bushes now on the west bank were on the east bank before the earthquake. Photo by T. McCrink, 4/9/10.

A *B*

Figure 91. *A,* Arcuate lateral spread fissures and *B*, vented sand near the eastern extent of the lateral spread at Rice Drain No. 3 (D12). Photos by T. McCrink, 4/9/10.

Samples of sand vented on the surface and material that flowed into one of the major cracks were collected, and grain size analyses are presented in appendix A (Sample IDs IMC–163 and IMC–164, respectively).

Cook Drain along Fites Road (D15)

The northernmost inferred liquefaction was found as a slump into Cook Drain along Fites Road, approximately 350 m east of where Urquhart and West Carter roads intersect. This location is adjacent to the southeast levee of the Westside Main Canal, and the surface of Fites Road is approximately 2 m lower than the levee top. The slump extended along Cook Drain for 40 to 50 m, dropped the edge of Fites Roads as much as 1 m, and the toe of the slump in two places flowed across the width of the drain channel impeding water flow (fig. 92). The slump corresponded to a stretch of the Westside Main Canal levee that was wet and had enough seepage to create a puddle on Fites Road (fig. 93). A road caution sign was lying on the ground near the puddle water on Fites road and showed indications of having been there for a long time, suggesting that seepage at this location has been prevalent for a while. The correspondence of the seepage zone with the slump and the morphology of the slump itself suggest that seepage extended beneath Fites Road, creating the opportunity for liquefaction to contribute to the triggering of the slump.

Major Facilities and Earthen Dams

Rio Bend RV Park Lake (F01)

A small man-made lake at the Rio Bend recreational vehicle (RV) Park experienced two small bank failures, which may be related to liquefaction, and some clearly liquefaction-related lateral spreading on the southwest side of the lake. The small bank failures occurred on the north and south sides of the lake, and on the east side where the lake narrows and is crossed by a bridge. Both features are suggestive of having been caused by liquefaction, but no vented sand was observed (fig. 94). Maximum extensional displacement was measured at roughly 52 cm. Lateral spreading with associated vented sand was observed at the edge of pavement near the southwest side of the lake, and similarly oriented small cracks were observed in the asphalt pavement (fig. 95). Separation amounting to less than a centimeter was observed between the asphalt and a concrete verge on the south side of the deformed pavement.

A *B*

Figure 92. *A,* View to northeast showing probable lateral spread ground failure into Cook Drain along Fites Road (D15). Wet sediment noted on west side of the road is believed to be seepage from Westside Main Canal, located to the left of the photo. Slump displacement is to the right; it visibly narrows the channel in the middle of the image. *B*, View of toe of slope failure where it partially blocks flow within the Cook Drain. Ground failure narrowed the channel at two different points along the zone. Photos by J. Tinsley, 4/8/10.

A *B*

Figure 93. *A,* Overview of southeast levee confining the Westside Main Canal adjacent to Fites Road, showing minor extensional cracking at the outer edge (D15). Extensional cracking extended for a fraction of the length of the slope failure adjacent to the drainage channel at left. No vented liquefied materials were observed along the Westside Main Canal levee. *B*, View to southwest along Fites Road showing seepage from the Westside Main Canal, which created a puddle of standing water on Fites Road. Photos by J. Tinsley, 4/8/10.

Sunbeam Lake Dam and Drew Road (F02, R12)

Sunbeam Lake, a recreational lake operated by Imperial County Division of Parks and Recreation, is located on Drew Road, approximately halfway between the town of Seeley and Interstate Highway 8. The lake itself is a narrow body of water, averaging about 70 m wide, that extends about 1.8 km from Drew Road southeast to Interstate Highway 8 (fig. 96). A small extension of the lake continues to the south side of the interstate highway, presumably by way of a

A *B*

Figure 94. Bank failures around Rio Bend RV Park Lake (F01). *A,* Bank failure on the north side of the lake. *B*, Bank failure on the south side. This failure extended underneath the footbridge seen in the distance. Photos by J. Tinsley, 4/7/10.

A *B*

Figure 95. Liquefaction lateral spread at the southwest side of the Rio Bend RV Park Lake (F01). *A,* View to the west; deformed asphalt pavement and adjacent fence. Liquefied fine silty sand vented from fracture that opened along northern limit of paving. *B*, View to the east showing en echelon extensional cracks in asphalt pavement and the open extensional fissures at the left of photo. Photos by J. Tinsley, 4/7/10.

culvert. The park ranger reported that the lake ranges from 3 to 5 m in depth. Owing to the relatively shallow lake depth and low relief of the area, the Sunbeam Lake Dam is only about 5 m above the lake outflow into the Seeley Drain on the west side of Drew Road.

Earthquake shaking from the mainshock on April 4 caused liquefaction of the dam crest, of the gently sloping embankment between the dam crest and Drew Road, and in Drew Road fill materials (fig. 97). The Sunbeam Lake park ranger witnessed water geysering through the asphalt surface of Drew Road, and photographs taken soon after the earthquake show both settlement and lateral displacement of the road (fig. 98). Unfortunately, the road had been leveled with dirt by the time any postearthquake investigators arrived, and no displacement could be measured. The road fill above the outlet pipes was washed away by water flow through the embankment soon after the earthquake (fig. 99), exposing several types of utilities and breaking at least one of them. It was reported that a gas main was also located in the roadbed on the east side of Drew Road.

The south half of the dam crest settled vertically between 15 and 30 cm and the upstream face spread toward the lake (figs. 100, 101 and 102*A*). Arcuate cracks at the north end of the dam

Figure 96. Location map of Sunbeam Lake, Imperial County (F02, R12). The dam is located at the far west end of the lake near Drew Road. The town of Seeley is at top left of image. Base Image is from Google Maps.

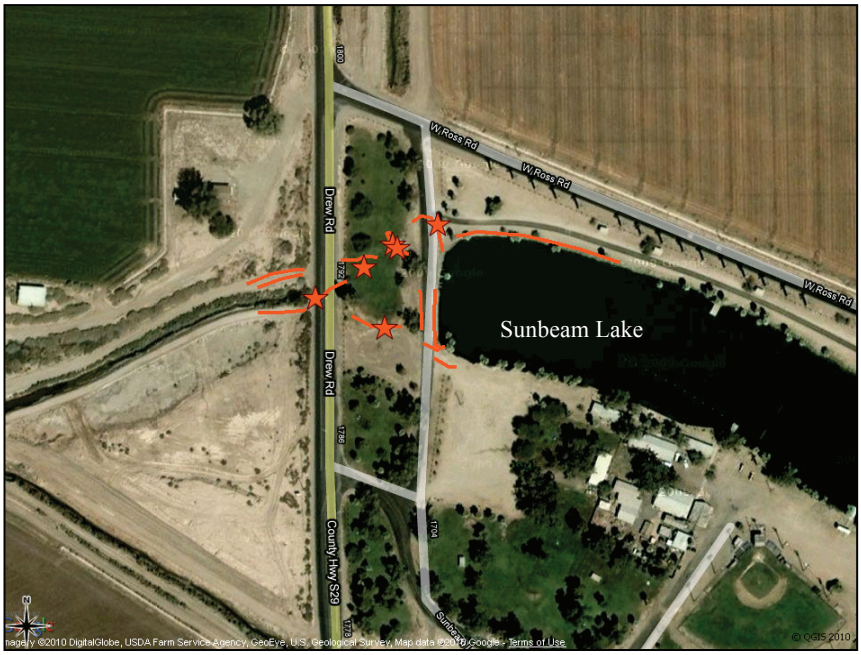

Figure 97. Diagrammatic representation of the damage observed at Sunbeam Lake Dam and Drew Road (F02, R12). Lines represent approximate areas where fissures and cracks were observed, and stars show the approximate locations of sand boils. Base image is from Google Maps.

Figure 98. Liquefaction-related settlement and lateral spreading of Drew Road, immediately west of Sunbeam Lake Dam (R12). View is toward the south with El Centinela Peak in the distance. An eyewitness reported water geysering out of the pavement during the earthquake. Outlet pipes from Sunbeam Lake and from a large irrigation drain enter the stream to the right of the prominent slump in the center-right of the photo, indicated by the arrow. Both apparently were damaged by liquefaction. Photo taken 4/4/10; courtesy of the Imperial County Planning and Development Services Department.

Figure 99. Close-up of the slump on the west side of Drew Road mentioned in the previous photo (R12). Several utility lines are exposed and some are broken. The outlet flow from Sunbeam Lake and probably the Seeley irrigation drain are just visible on the right. Photo courtesy of Imperial County Planning and Development Services Department.

crest indicated lateral spreading to the west. East-west-trending cracks on the south side of the gentle slope between the dam crest and Drew Road showed westward displacements of about 4 cm. Cracks on the north side of this slope were displaced vertically as much as 10 cm. Vented sand was observed at several locations on this grassy slope in proximity to the cracks, and in association with the arcuate cracks on the north end of the dam crest (fig. 97). A sample of the vented sand was collected, and grain-size analysis is presented in appendix A (Sample ID IMC–160).

Liquefaction-related settlement and lateral spreading of the dam crest disrupted the outlet pipes near the lake outflow weir structure. Water flowing outside of the pipes and through the

Figure 100. View of the south end of the Sunbeam Lake Dam crest, looking east (F02). Photo was taken soon after the earthquake. Dam crest to the left has dropped 15 to 30 cm relative to the area to the right of the large crack in the center of the photo. Photo courtesy of Imperial County Planning and Development Services Department.

Figure 101. View of the south end of the Sunbeam Lake Dam crest, looking northeast (F02). Photo was taken 8 days after the earthquake. Transverse crack on the crest is larger and new cracks parallel to it are now visible. Cracks in asphalt are more pronounced and several newly visible cracks extend into the lawn area. The continued deformation may be the result of a week of strong aftershocks. Photo by T. McCrink, 4/12/10.

embankment began piping away embankment soils leading to the development of a sinkhole on the dam crest (fig. 102). After a week, the sinkhole had grown to an estimated 15 m^3 depression on the top of the dam and threatened its integrity. On April 20, 2010, after field work had ceased, the assistant director for Imperial County Public Works informed one of the authors of this report (McCrink) that the dam outlet had been repaired by excavating to a depth of 6 m and replacing three sections of pipe (fig. 103). On June 8, 2010, McCrink had the opportunity to revisit the Sunbeam Lake dam and found repairs included those described by the county to the outlet, placement of concrete rubble on the upstream side of the dam, repairs to the outlet pipe on the west side of Drew Road, and regrading of the dirt access roads on both sides of the drain west of Drew Road. However, as of September 15, 2010, Drew Road was still closed and waiting for repairs.

Figure 102. Time sequence photographs of a sinkhole that formed on the Sunbeam Lake Dam (F02). *A*, The dam crest and outlet weir on the day of the earthquake. Photo courtesy of Imperial County Planning and Development Services Department. *B*, Early stage of sinkhole formation on the morning of 4/7/2010; the person whose shadow partly covers the sinkhole is standing on the outlet weir. Photo by J. Tinsley. *C*, Sinkhole on the evening of 4/8/2010. Photo by T. McCrink. *D*, Sinkhole on 4/12. Photo by T. McCrink.

Because liquefaction and related deformation was evident throughout the area between the lake and Drew Road, it seems likely that this area is susceptible to future liquefaction deformation.

Seiching was also observed at Sunbeam Lake Park. According to the county's park ranger, the swimming pool on the south side of the lake sloshed enough water to flood the surrounding picnic areas and nearby restrooms (fig. 104). In addition, the banks of the lake are shown to be wet in photographs taken by Imperial County personnel in the evening after the earthquake (fig. 105). In order to wet the banks of the lake, seiche waves had to be locally on the order of half a meter high.

All American Canal Aqueduct over the New River (F03, R15)

The All American Canal crosses the New River through a closed aqueduct system composed of two approximately 4-m-diameter pipes, which are elevated above the riverbed by four massive, rectangular concrete supports (fig. 106). By April 10, 2010, when the site was visited, much of the flat floodplain area of the New River had been graded. However, considerable evidence of liquefaction in this area was still observed. A 30-m-wide lateral spread slump were seen on the south bank of the New River 150 m upstream from the aqueduct. Sand boils were found in nearly all flood plain areas left ungraded around the aqueduct, particularly underneath and west of the structure. Vented sand was characterized by very fine grained ejected material, often displaying shrinkage cracks, in relatively small volumes (fig. 106). At the base of one concrete support, a linear string of these fine-grained sand boils paralleled the support structure, suggesting

Figure 103. Repairs to Sunbeam Lake Dam and Drew Road as of June 8, 2010 (F02). *A,* Outlet weir and dam crest where sinkhole used to be. Note that barricades are still blocking Drew Road in the distance. *B*, View of water flowing over the weir and through the outlet pipe. *C*, Concrete rubble has been placed on the upstream side of the dam crest. Note that the lamp post is still leaning toward the lake as a result of the now-obscured lateral spreading. *D*, Repaired outlet pipe on the west side of Drew Road. Photos by T. McCrink, 6/8/10.

Figure 104. Standing water resulting from earthquake-generated seiche waves at Sunbeam Lake Park (F02). *A,* Photograph of the swimming pool south of Sunbeam Lake. Wet area shows the extent of the water that sloshed out of the pool. *B*, Picnic area adjacent to the pool flooded by water sloshed out of the pool. Photos courtesy of Imperial County Parks and Recreation; taken 4/410.

Figure 105. Photograph of the south bank of Sunbeam Lake (F02). Wet areas, shown as dark soil at the edge of the dirt path, indicates where water splashed out of the lake. The steep sides of the bank are on the order of 0.5 m high. Photo courtesy of Imperial County Parks and Recreation; taken 4/4/10.

A *B*

Figure 106. Liquefaction vented sand near the All American Canal aqueduct over the New River (F03). Relatively low volumes of fine-grained ejected material characterize the sand boils in this area. *A,* View of vented sand on the New River flood plain, looking northeast toward the aqueduct. Photo by C. Pridmore, 4/10/10. *B*, Close-up of vented sand. Photo by T. McCrink, 4/10/10.

some influence of the structure on liquefaction at this location (fig. 107). A timber bridge crossing the New River east of the aqueduct (R15) was closed on April 10, 2010, but the damage that caused the closure was not readily discernible.

Calexico Waste Water Treatment Plant (F04, D14)

The Calexico Waste Water Treatment Plant is located at the southwest corner of the City of Calexico, on the south bank of the New River and immediately north of Calexico International

Airport (fig. 108). Extensive liquefaction-related deformation was observed on the plant access road east of the airport, resulting in the closure of the road, and on the west side of the plant where liquefaction lateral spreading damaged embankments that impound partially solidified sludge and gray water. Lateral spreading fissures also were observed traversing sludge ponds near the central area of the plant. The UCLA team found liquefaction-induced lateral spreads and associated vented

A *B*

Figure 107. Liquefaction sand boils near the base of one All American Canal aqueduct support structure (F03). *A,* Line of sand boils parallel to the support structure. Photo by C. Pridmore, 4/10/10. *B*, Close-up of the vented fine sand. Note desiccation cracks forming in ejected material. Photo by T. McCrink, 4/10/10.

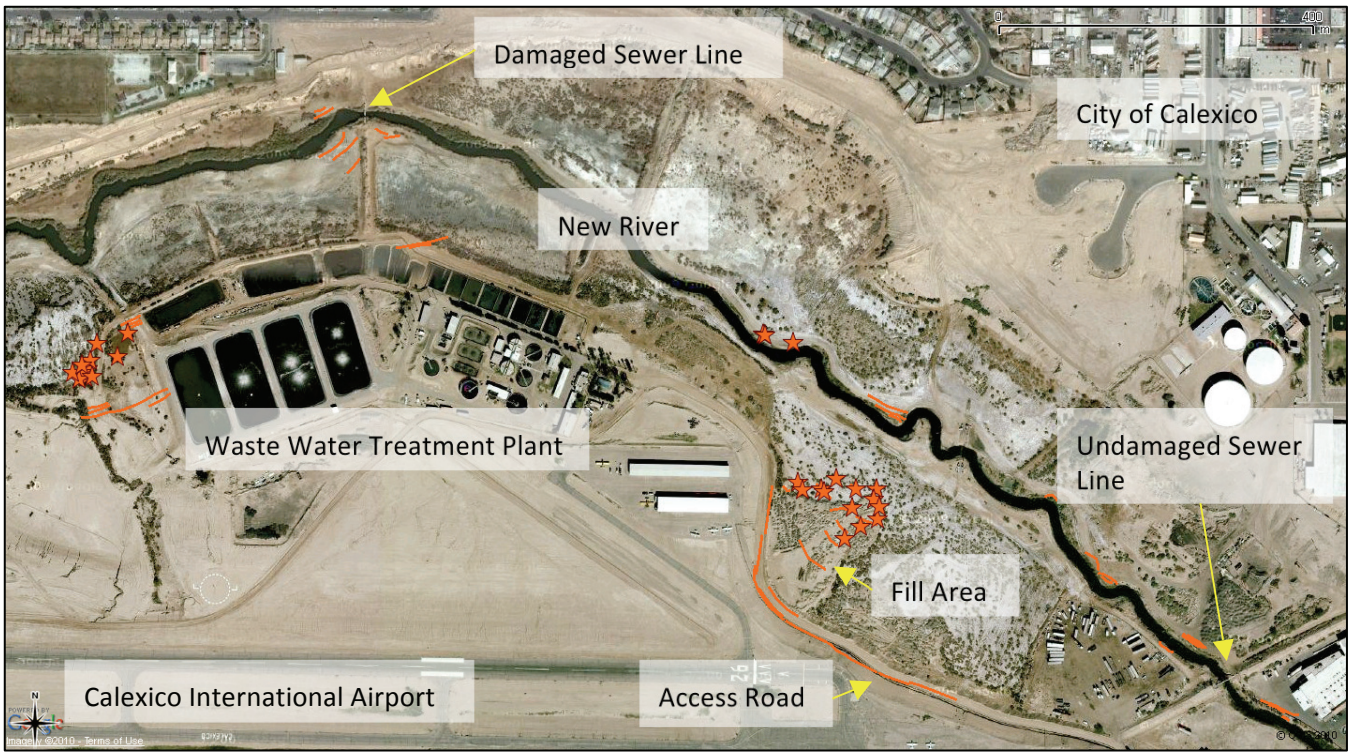

Figure 108. Map of liquefaction features at the Calexico Waste Water Treatment Plant and New River Floodplain (F04). Liquefaction-related ground deformation severly affected the access road on the east side of the plant, and fissuring observed on the west side and central area may extend into ponds. Lines represent approximate observed fissure locations; stars represent approximate observed sand boil locations. Base image is from Google Maps.

sand on the north bank of the New River east of the Waste Water Treatment Plant on April 5, 2010. At the time of the California Geological Survey team's visit on April 10, 2010, crews were actively engaged in reconnecting a 91-cm-diameter sewer trunk line broken where it crosses the New River. Lateral spread fissures were observed on the north and south New River flood plain in this area, but the cause of the broken sewer line was not determined.

Liquefaction damage to the access road extends for a distance of about 350 m with the greatest damage in the central portion where the road curves. Cumulative vertical displacement on the inboard (southwest) side of the road may be as much as 1 m maximum, and horizontal displacement is on the order of 20 to 30 cm (figs. 109 and 110). No evidence of slump and spread movement at the base of the road embankment was found along the southeast half of the damaged access road, perhaps because it was masked by rubble piles. Additionally, no evidence of cracking or sand boils was observed on the flood plain immediately northeast. Damage to the outboard (east-northeast) side of the road was not apparent except where the road adjoins a large nonengineered fill lying to the east-northeast (fig. 108). Here, uphill-facing scarps with less vertical displacement than on the inboard side indicate both settlement and rotation of the road fill prism. Geotextile was found in road base beneath asphalt in an exposed crack on the northeast side of the road, and this may explain why the pavement did not experience the same intensity of damage as the sides of the road. It was reported that this road was reconstructed and paved in the last four years.

Extensional cracks were found thoughout most of the fill area, and numerous sand boils were seen toward the northeast where the fill thins (fig. 111). On the flood plain north and east of the fill, numerous fissures and related sand boils were found (fig. 112).

The west side of the waste water treatment plant is characterized by extensive areas of sand boils and lateral spread cracks (figs. 113 through 116). Sand boils appear confined to floodplain areas, though considerable volumes of sand were ejected. Lateral spread fissures occur on the floodplains associated with sand boils and extend into and through fill areas, including pond embankments at the plant.

Figure 109. Liquefaction lateral spread and slump of waste water treatment plant access road (F04). A matching but smaller uphill-facing scarp on the other side of the road indicates that the soil under the pavement settled and rotated. Geotextile was observed in exposed road base, which may have helped keep pavement from experiencing the intensity of fissuring observed on the sides of the road. View to the west. Photo by T. McCrink, 4/10/10.

On the New River floodplain east and north of the waste water treatment plant, liquefaction lateral spreading features were observed from just south of the Anza Road (West 2nd Street) bridge to west of the large sewer line damaged by the earthquake (fig.108). These features ranged from incipient spreading cracks with minor displacements to larger slumps and associated vented sand.

Figure 110. Liquefaction lateral spread and slump of waste water treatment plant access road (F04). A portion of the hill, probably fill, also experienced slumping. View to the southeast. Photo by T. McCrink, 4/10/10.

Figure 111. Liquefaction vented sand and related cracking in nonengineered fill adjacent to the Treatment Plant access road (F04). Access road is at the base of the hill in the distance and the airport is just beyond. View to the southwest. Photo by C. Pridmore, 4/10/10.

Figure 112. Liquefaction sand boils and fissures on the New River flood plain, just north of the nonengineered fill along the Treatment Plant access road (F04). Stains on sand boils are thought to be salts contained in the groundwater that turn white upon drying. Most sand boils were wet in this area, and are believed to have been reactivated by a M4.4 aftershock that occurred the night before. View to the north. Photo by C. Pridmore, 4/10/10.

Figure 113. Extensive vented sand flooding areas between bushes on the New River floodplain west of the waste water treatment plant (F04). View to the west. Photo by T. McCrink, 4/10/10.

Figure 114. Lateral spread fissures extending through sludge drying ponds on the west side of the waste water treatment plant (F04). Fissure in the foregound is extensional and those in the middle of the picture show vertical displacement on the order of 2 to 5 cm. View to the southeast. Photo by T. McCrink, 4/10/10.

Figure 115. View to the southeast of a large scarp at the head of a liquefaction lateral spread on the west side of the Calexico Waste Water Treatment Plant (F04). Cumulative vertical displacement is about 1 m. Photo by T. McCrink, 4/10/10.

Figure 116. Liquefaction lateral spread fissures extending across New River flood plain into pond embankments on the west side of the Waste Water Treatment Plant (F04). Arrows point to fissures in the embankment. At the time of the California Geological Survey visit, a track-mounted excavator (orange machine arm in the top center of this photo) was making repairs in the center of the plant at a point suspiciously in line with these fissures. View to the east from the large scarp shown in figure 115. Photo by T. McCrink, 4/10/10.

Concluding Remarks

Liquefaction caused by the M7.2 El Mayor–Cucapah earthquake was widespread throughout the southern Imperial Valley but concentrated in the southwest corner of the valley, southwest of the city centers of Calexico and El Centro, where recorded ground motions were highest. Although there are few strong motion recordings in the very western part of the area, the recordings that do exist indicate that ground motions were on the order of 0.3 to 0.6 g where the majority of liquefaction occurrences were found. More distant liquefaction, at Fites Road southwest of Brawley and along Rosita Canal northwest of Holtville, were triggered where ground motions were about 0.2 g. Liquefaction at these locations likely was facilitated by shallow groundwater resulting from pre-earthquake seepage from the Westside Main and Rosita canals, respectively. Identifying and repairing areas where seepage is developing may limit future earthquake damage to canals.

The frequency and intensity of damage generally decreased to the north and east, away from the earthquake epicenter and the main sediment source, the Colorado River. This trend likely reflects the attenuation of strong ground motion with increasing distance from the earthquake source as well as a tendency for natural deposits to increase their content of fines (silt and clay) away from the Colorado River. One occurrence of liquefaction and lateral spreading in an agricultural field documented in this reconnaissance appears to be related to the absence of tile drains. Tile drains are common features to most agricultural fields in Imperial County, where few fields experienced liquefaction, but are less common in the Mexicali Valley where extensive liquefaction-related damage was observed. The extent to which tile drains reduce surface manifestations of liquefaction and under what conditions should be studied further.

Damage to roads was associated mainly with liquefaction of sandy river deposits beneath road fills, and in some cases liquefaction within the fills. Liquefaction damage to canal and drain levees was not always accompanied by vented sand, but the nature of the damage leads the authors to infer that liquefaction was involved in the majority of observed cases. Liquefaction-related damage to several public facilities, the Calexico Waste Water Treatment Plant, and the Sunbeam Lake Dam in particular, appears to be extensive. The cost to repair these facilities to prevent future liquefaction damage will likely be prohibitive. As such, it is likely that liquefaction will recur at these facilities during the next large earthquake.

One of the more interesting liquefaction occurrences from this earthquake is that at the levee between Fig Lagoon and the New River. The observations at this location reveal a sequence of events that include liquefaction, lateral spreading and slumping, seiche wave generation, overtopping of the compromised levee, and subsequent liquefaction triggered by aftershocks. It is rare that the timing of these events is so completely recorded.

Few sites that experienced liquefaction during the El Mayor–Cucapah earthquake experienced liquefaction in previous earthquakes in the Imperial Valley. Liquefaction at the Worthington Road crossing of the New River, the furthest north found along the New River in this reconnaissance also was reported at this location during the 1968 Borrego Mountain and 1987 Superstition Hills earthquakes (Castle and Youd, 1972; Meehan and others, 1988). Inferred liquefaction-related slumping along the Westside Main Canal triggered by this earthquake occurred in similar areas with similar styles of deformation as failures reported from the 1987 Superstition Hills earthquake (Finch, 1988). Finally, extensive cracking and slumping along the All American Canal at the Alamo River crossing observed in this reconnaissance was also reported during the 1979 Imperial Valley and the 1987 Superstition Hills earthquakes (Youd and Wieczorek, 1982; Finch, 1988).

The Wildlife Liquefaction Array did not experience ground motions high enough during the El Mayor–Cucapah earthquake to initiate liquefaction. A number of sites where liquefaction was triggered during the 1979 Imperial Valley earthquake were visited during this reconnaissance. None of the visited sites were found to have experienced a repeat of liquefaction from this earthquake. The lack of documented repeat liquefaction occurrences from the 1979 Imperial Valley earthquake is most likely due to the greater distance of the El Mayor–Cucapah earthquake. As such, it seems likely that sites that liquefied in 1979 could again liquefy with a repeat of a large earthquake along the Imperial fault.

This postearthquake liquefaction reconnaissance was fairly comprehensive in its scope, but the liquefaction occurrences documented here should be considered just a sample of the total. Because the focus of the reconnaissance was on easily accessed areas, such as roads and levees, it is more than likely that numerous liquefaction occurrences were not observed, particularly along stretches of the New River inaccessible to vehicles. In addition, many ground failure locations along irrigation canals and drains were under repair within days of the earthquake, owing to the economic significance of these facilities to the local agricultural industry. This rapid repair highlights the importance of mobilizing crews to map liquefaction effects soon after an earthquake event, and it also means that some evidence of liquefaction was obliterated prior to being visited.

Most large earthquakes reveal weaknesses to the built environment, and the El Mayor–Cucapah earthquake is no exception. Liquefaction-related damage to two engineered earth structures came very close to releasing large volumes of water into the New River, which may have threatened bridges and agricultural facilities downstream. First, the overtopping of the levee between Fig Lagoon and the New River could have completely breached the levee releasing a very large volume of water into the New River. Second, postearthquake piping around the liquefaction-damaged outlet of the earth dam at Sunbeam Lake threatened to undermine the dam and drain the lake into the New River, possibly breaking several important utilities buried along Drew Road in the process. Repairs to these facilities appear to have been appropriately focused on resolving the immediate threats. However, repairs that do not improve the resistance to liquefaction potential at these and other sites leave them open to repeated failures in future earthquakes.

Finally, researching historic earthquakes in and around Imperial Valley made it apparent that a repeat of the 1940 rupture of the Imperial fault poses a serious threat to the communities in the valley. When the 1940 Imperial fault surface rupture displaced the All American Canal levees by 5 m, the canal was still under construction and not yet transporting water. A repeat of that rupture could cut off the water supply to the many cities in Imperial Valley and the agricultural industry that supports them.

Acknowledgments

The authors are indebted to Socrates Gonzalez, Imperial Irrigation District, for advice, insights, and access to District facilities. UCLA Students Dong Youp Kwak, Emel Seyhan, Walter Lopez, and Lisa Star assisted with the investigation on April 5, 2010. Luis Pacheco, Darrel Garner, and Jung Hueberger, Imperial County Planning and Development Services Department, provided verbal accounts of the evolution of permanent ground deformation at Sunbeam Park, Sunbeam Lake Dam, and nearby infrastructure, and generously provided copies of photographs taken within hours after the earthquake. Robert Anderson and Fred Turner with the California Seismic Safety Commission relayed their observations and reports of ground failures to the California Geological Survey and U.S. Geological Survey teams while reconnaissance was being conducted. Michael J. Bennett and Coyn Criley of the U.S. Geological Survey performed the index testing on vented liquefied sediment contained in appendix A of this report. Thomas Fumal and Thomas L. Holzer of

the U.S. Geological Survey and Chris Wills of the California Geological Survey provided timely and insightful reviews of the manuscript.

References Cited

American Society for Testing and Materials, 1983, Annual book of ASTM standards, Soil and rock; Building stones, section 4: American Society for Testing and Materials, Philadelphia, Pa., 734 p.

Beal, C.H., 1915, The earthquake in the Imperial Valley, California, June 22, 1915: Bulletin of the Seismological Society of America, v. 5, p. 130–149.

Bennett, M.J., and Tinsley, J.C., III, 1995, Geotechnical data from surface and subsurface samples outside of and within liquefaction-related ground failures caused by the October 17, 1989, Loma Prieta earthquake, Santa Cruz and Monterey counties, California: U.S. Geological Survey Open-File Report 95–663, 358 p.

Blake, William P., 1857, Geological report, *in* Williamson, R.S., Report of explorations in California for railroad routes to connect with the routes near the 35th and 32nd parallels of north latitude: Washington, D.C., Government Printing Office, 310 p.

Brothers, D.S., Driscoll, N.W., Kent, G.M., Harding, A.J., Babcock, J.M., and Baskin, R.L., 2009, Tectonic evolution of the Salton Sea inferred from seismic reflection data: Nature Geoscience, v. 2, p. 581–584.

Castle, R.O., and Youd, T.L., 1972, Engineering geology, *in* The Borrego Mountain earthquake of April 9, 1968: U.S. Geological Survey Professional Paper 787, p. 58–174.

Cory, H.T., and Blake, W.P., 1915, The Imperial Valley and the Salton Sink: John J. Newbegin, San Francisco, 1,581 p.

Ellsworth, W.L., 1990, Earthquake history, 1769–1989, *in* Wallace, R.E., ed., 1990, The San Andreas fault system, California: U.S. Geological Survey Professional Paper 1515, p. 153–181.

Finch, M.O., 1988, Damage to irrigation facilities in Imperial Valley, Superstition Hills earthquakes of November 1987: California Geology, v. 41, no. 4, p. 85–90.

Google Maps base images, 2010, accessed at *http://maps.google.com/maps*. Last accessed 20 November 2010.

Holzer, T.L., Youd, T.L., and Hanks, T.C., 1989, Dynamics of liquefaction during the 1987 Superstition Hills, California, earthquake: Science, v. 244, p. 56–59.

Holzer, T.L., and Youd, T.L., 2007, Liquefaction, ground oscillation, and soil deformation at the Wildlife Array, California: Bulletin of the Seismological Society of America, v. 97, no. 3, p. 961–976.

Hough, S.E. and Elliot, A., 2004, Revisiting the 23 February 1892 Laguna Salada earthquake: Bulletin of the Seismological Society of America, v. 94, no. 4, p. 1571–1578.

Howard, A.K., 1984, The revised ASTM standard on the Unified Soil Classification System: Geotechnical Testing Journal, v. 7, no. 4, p. 458–482.

Meehan, Jack, Hart, E., and Schiff, A., 1988, Superstition Hills earthquakes—November 23 and 24, 1987, Imperial County, California: Earthquake Engineering Research Institute Newsletter, v. 22, no. 2, 8 p.

Mendenhall, W.C., 1909. Ground waters of the Indio region, California: U.S. Geological Survey Water-Supply Paper 225, 56 p.

Merriam, R. H. and Bandy, O.L., 1965, Source of upper Cenozoic sediments in Colorado delta region: Journal of Sedimentary Petrology, v. 35, p. 911–916.

Mueller, K.J., and Rockwell, T.K., 1995, Late Quaternary activity of the Laguna Salada fault in northern Baja California, Mexico: Geological Society of America Bulletin, v. 107, p. 8–18.

National Agricultural Imagery Program [NAIP], 2005, for Imperial County, California, accessed at *http://www.atlas.ca.gov/download.html#/casil/imageryBaseMapsLandCover/imagery/naip/naip_2005/county_mosaics/Imperial* . Last accessed 20 November 2010.

Seed, H.B., and Idriss, I.M., 1982, Ground motions and soil liquefaction during earthquakes: Oakland, Calif., Earthquake Engineering Research Institute, 134 p.

Sharp, R.V., 1981, Variable rates of late Quaternary strike slip on the San Jacinto fault zone, southern California: Journal of Geophysical Research, v. 86, no. B3, p. 1754–1762.

Stover, C.W., and Coffman, J.L., 1993, Seismicity of the United States, 1568–1989 (rev.): U.S. Geological Survey Professional Paper 1527, 418 p.

Strahorn, A.T., Watson, E.B., Kocher, A.E., Eckmann, E.C., and Hammon, J.B., 1922, Soil survey of the El Centro area, California: U. S. Department of Agriculture.

Sylvester, A. G., 1979, Earthquake damage in Imperial Valley, California May 18, 1940, as reported by T.A. Clark: Bulletin of the Seismological Society of America, v. 69, no. 2, p. 547–568.

Ulrich, F.P., 1941, The Imperial Valley earthquakes of 1940: Bulletin of the Seismological Society of America, v. 31, no.1, p. 13–32.

U.S. Geological Survey, 2010, Magnitude 7.2 Baja California, Mexico, earthquake information available at *http://earthquake.usgs.gov/earthquakes/eqinthenews/2010/ci14607652/.* Last accessed 20 January 2011.

Youd, T.L., and Wieczorek, G.F., 1982, Liquefaction and secondary ground failure, *in* The Imperial Valley, California, earthquake of October 15, 1979: U.S. Geological Survey Professional Paper 1254, p. 223–246.

Youd, T.L., and Wieczorek, G.F., 1984, Liquefaction during the 1981 and previous earthquakes near Westmorland, California: U.S. Geological Survey Open-File Report 84–680, 36 p.

Zelwer, Reuben, and Grannell, R.B., 1982, Correlation between precision gravity and subsidence measurements at Cerro Prieto, *presented at* Cerro Prieto Geothermal Field Symposium, 4th, Guadalajara, Mexico, 1982: Lawrence Berkeley Laboratory LBL–14894, Cerro Prieto–22, p. 1–7.

Appendix A

Appendix A contains particle size distribution data from vented "sand-blow" samples collected by USGS and California Geological Survey field personnel in the Imperial Valley during field investigations of liquefaction triggered by the El Mayor–Cucapah earthquake.

Five samples of silty sand and sandy silt were collected from four locations where materials had vented to the ground surface from a liquefied substrate. The liquefied materials were either from placed fill that had liquefied or from natural deposits that had liquefied from beds underlying placed fill. It is not known precisely what the provenance of the vented sand may be at each locality without conducting a site-specific subsurface study at each site; such site- specific work is beyond the scope of this reconnaissance investigation. Index tests conducted in the laboratory on these five soil samples were grain size analyses using sieves and hydrometers (D422–63; American Society for Testing and Materials, 1983) in order to classify and describe the material according to the Unified Soil Classification (USC) (D2488–69, ASTM, 1983) as modified by Howard (1984). Table A1 lists the samples, the waypoint nearest the sample, and the particle size data and Unified Soil Classification (USC) designation for each sample.

The D_{50} or 50^{th} percentile particle size values for the sand samples range between 0.06 and 0.09 mm, spanning the fine sand to coarse silt range; no gravel clasts occurred in these samples. We note the sample IMC-164 from the "flowing fissure fill" collected by one of us (McCrink) was unusually high in clay (16% by weight), a value at or just above the empirical limit at which geotechnical opinion deems sediment to be too cohesive to liquefy. The issue is discussed more completely by Seed and Idriss (1982, p. 111-113). The particle size ranges collected are described in the USC as silty sand and sandy silt; both types of soil are commonly found comprising vented sediment during postearthquake liquefaction studies (for example, see Bennett and Tinsley, 1995).

Table A1. Grain size characteristics of vented liquefied soil, Imperial Valley, El Mayor–Cucapah earthquake, 4/4/2010.

[D_{50}, 50th percentile particle size in mm; Cu, coefficient of uniformity; USC, "Unified Soil Classification"; SM, silty sand; MLS, sandy sil

Site ID	Sample ID	Field Sample number	Depth interval, m	Gravel >4.75 mm	Sand 4.75-0.075 mm	Silt 0.075-0.005 mm	Clay <0.005 mm	D_{50} mm	Fines, <0.075 mm	Cu D_{60}/D_{10}
F02	IMC-160	JT-201000407-1	Surface	0	60	36	4	0.085	40	2.3
C29	IMC-161	JT-20100407-2	Surface	0	43	54	3	0.071	57	2.2
R18	IMC-162	JT-20100408-1	Surface	0	81	17	2	0.114	19	2.2
D12	IMC-163	CGS021- vented sand	Surface	0	37	55	8	0.065	63	72
D12	IMC-164	CGS021- fissure fill	Surface	0	54	30	16	0.080	46	

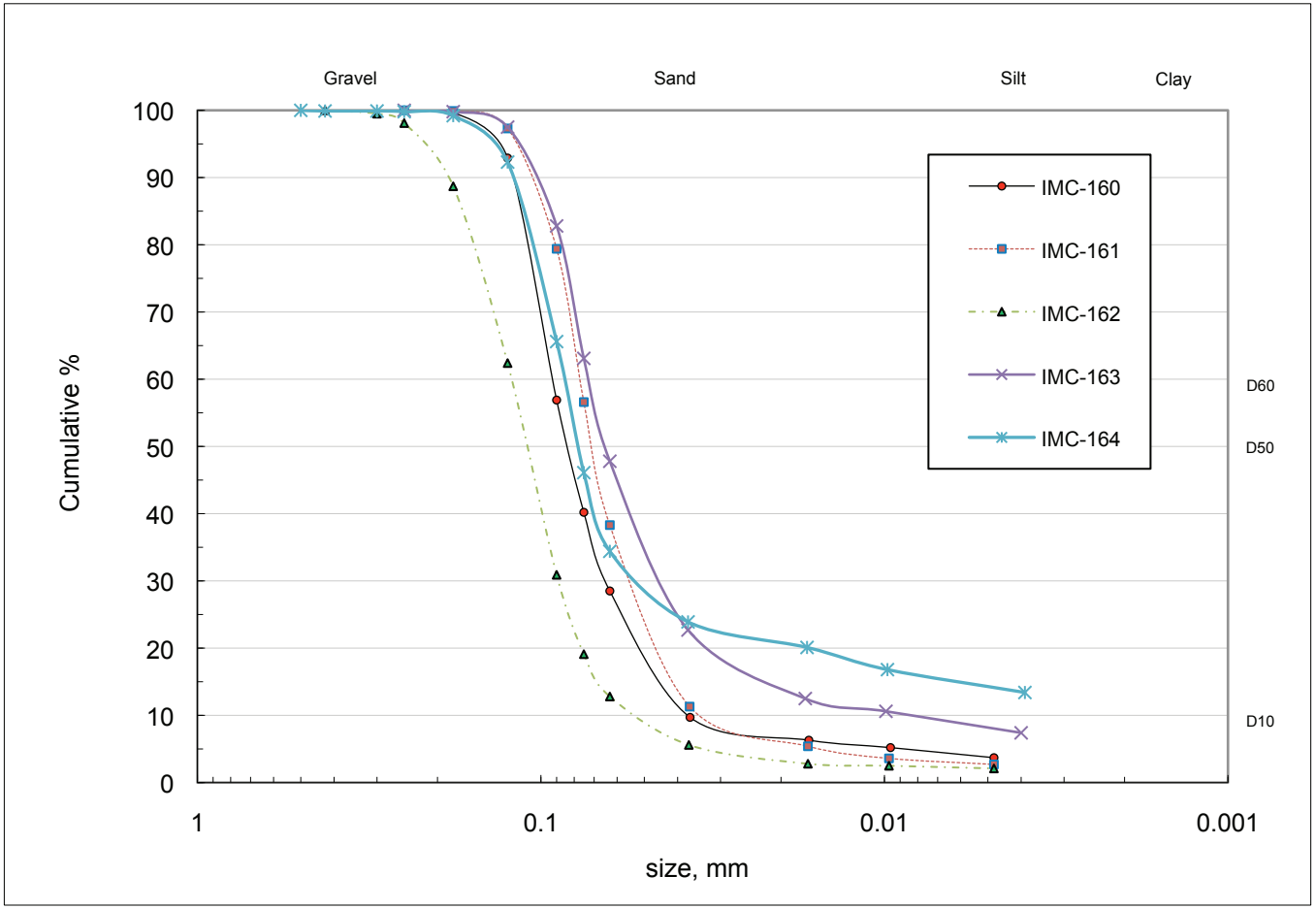

Figure A1. Cumulative percent particle-size curves for samples IMC160 through IMC 164 are shown as weight % versus particle size in mm. Soils are silty sand and sandy silt, a particle size range commonly observed in materials vented during earthquake-triggered liquefaction.